Graphical Abstract

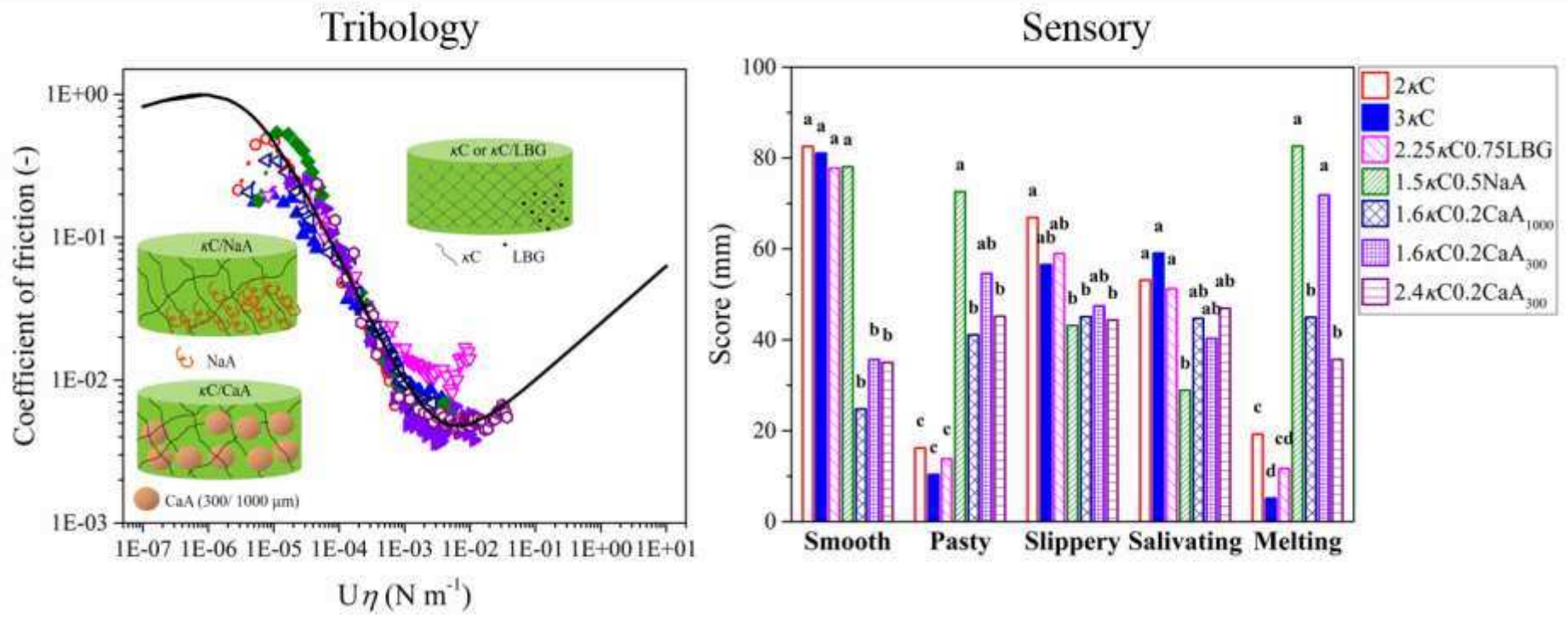

Highlights

- Oral processing of hydrogels was influenced by introducing structural inhomogeneity
- Correlations existed between chewing attributes and gel fracture, boli rheology
- Friction coefficient (μ) corroborated Stribeck master curve only in mixed regime
- 'Pasty' was inversely correlated with μ of bolus filtrate at orally relevant speed
- 'Salivating' correlated with initial fracture properties, boli rheology and tribology

On relating rheology and oral tribology to sensory properties in hydrogels

Emma M. Krop [a], Marion M. Hetherington [b], Melvin Holmes [a], Sophie Miquel [c], Anwesha Sarkar [a]*

[a] Food Colloids and Processing Group, School of Food Science and Nutrition, University of Leeds, Leeds LS2 9JT, United Kingdom

[b] School of Psychology, University of Leeds, Leeds LS2 9JT, United Kingdom

[c] Mars Wrigley Confectionery, 1132 West Blackhawk Street, Chicago, IL 60642, USA

*Corresponding author:

Dr Anwesha Sarkar

Food Colloids and Processing Group,

School of Food Science and Nutrition, University of Leeds, Leeds LS2 9JT, UK

E-mail address: A.Sarkar@leeds.ac.uk

Phone: +44 (0) 113 343 2748

Abstract

The aim of this study was to understand the relationship between rheological, tribological and sensory properties (n=11 panellists) of hydrogels differing in hydrocolloid type, concentration and degree of inhomogeneity. Fracture properties of hydrogels containing different ratios of *κ*-carrageenan (*κ*C) and/or locust bean gum (LBG), sodium alginate (NaA), 300/1000 μm calcium alginate beads (CaA) at 1-4 wt% concentration were determined. Viscosity and friction coefficients (μ) of the hydrogel-boli after simulated oral processing were characterized. Tribology measurements were conducted in a polydimethylsiloxane ball/disc set-up with pre-adsorbed artificial salivary film at 37 °C. 'Scaling' with boli viscosity showed good agreement of observed data with the Stribeck master curve, however only in the mixed regime i.e. at intermediate values of the product of velocity and lubricant viscosity ($U\eta$). Low μ values of gel boli in the boundary regime were largely driven by the formation of a viscous layer of bolus fragments between opposing surfaces. Fracture properties of hydrogels and boli viscosity were correlated with all chewing-related texture attributes i.e. 'firm', 'elastic', 'chewy' and 'cohesive' and inversely correlated with lubrication-related attributes 'melting' and 'pasty' ($p<0.05$). On the other hand, μ of the bolus filtrate at orally relevant speeds (50 mm/s) was inversely correlated with lubrication-related attributes 'pasty' and positively with 'slippery' ($p<0.05$). The lack of correlations with 'smooth' could be explained due to sample inhomogeneity and the absence of 'ball-bearing'-ability of the gel beads. A combination of initial fracture properties, boli viscosity and tribology of bolus filtrates (mixed regime) impacted the lubrication-related attribute 'salivating' ($p<0.05$).

Keywords

Oral processing; Sensory attributes; Texture; Bolus viscosity; Oral Tribology; Lubrication

1. Introduction

Oral processing strategies, such as higher number of chews and longer oral residence time have recently been linked to lower self-reported hunger and food intake in controlled experiments (Krop, et al., 2018; Miquel-Kergoat, Azais-Braesco, Burton-Freeman, & Hetherington, 2015). Hence, there has been a gradual increase in research efforts to understand and alter oral processing i.e. in-mouth chewing and lubrication by means of microstructural engineering (Laguna, Hetherington, Chen, Artigas, & Sarkar, 2016; Laguna & Sarkar, 2016). Understanding the characteristics of oral processing (chewing, lubrication) has drawn significant research attention with the focal point recently shifting from rheology to tribology. This is largely due to the current consensus on the transformation during oral processing from rheology (bulk property) to tribology (surface property of food-saliva bolus based lubricants) (Chen & Stokes, 2012; Garrec & Norton, 2013; Laguna & Sarkar, 2017; Pradal & Stokes, 2016; Prakash, Tan, & Chen, 2013; Sarkar, Kanti, Gulotta, Murray, & Zhang, 2017a; Stokes, Boehm, & Baier, 2013; van Stee, de Hoog, & van de Velde, 2017).

An important aspect of oral processing of solid and semi-solid foods is the incorporation of saliva to form a swallowable food bolus. Saliva is a complex biological fluid that consists of mainly water (~99.5%), various enzymes (α-amylase, lysozyme) and proteins, (~0.3%), small organic compounds and inorganic salts (Sarkar, Goh, & Singh, 2009; Sarkar & Singh, 2012; Sarkar, Ye, & Singh, 2017b). The key protein component in human saliva is highly glycosylated mucin, which mainly contributes to the lubrication and shear-thinning properties of saliva (Schipper, Silletti, & Vingerhoeds, 2007; Vijay, Inui, Dodds, Proctor, & Carpenter, 2015). The incorporation of saliva over time within a single bite episode has a major effect on the texture perception (Funami, Ishihara, Nakauma, Kohyama, & Nishinari, 2012; Hutchings & Lillford, 1988). The in-mouth friction properties might change significantly due to the interactions between food and salivary components, such as mucins and salts. However, few

studies have used real human saliva, or artificial saliva formulation, within in vitro oral processing experiments to understand its impact on the mechanical properties, such as viscosity or friction coefficient, and correlated such data to sensory perception (Laguna, Farrell, Bryant, Morina, & Sarkar, 2017a; Laguna, et al., 2017b; Morell, Chen, & Fiszman, 2017).

This study creates a unique body of evidence on the initial fracture properties of hydrogels, viscosity and tribology of hydrogel boli created using simulated oral processing (using artificial saliva formulation) and sensory profiling (descriptive analysis) to understand the relationship between mechanical and sensory properties. To investigate food oral processing, biopolymeric 'hydrogels' have been the choice as model solids and semi-solid foods in literature (Hayakawa, et al., 2014; Hori, et al., 2015; Kohyama, et al., 2015; Laguna, et al., 2016; Laguna & Sarkar, 2016; Santagiuliana, Piqueras-Fiszman, van der Linden, Stieger, & Scholten, 2018). This is because hydrogels have a relatively low level of complexity as compared to most composite foods systems. They can be structurally manipulated in a systematic manner, and exclude prior learning, emotional associations and expected postprandial satisfaction (if any) during sensory testing.

Recently, there has been an increase in research efforts directed towards designing hydrogels with structural complexity for various applications (Laguna & Sarkar, 2016; Santagiuliana, et al., 2018; Tang, Larsen, Ferguson, & James, 2016). For instance, Laguna & Sarkar (2016) demonstrated that incorporation of calcium alginate gel beads of 185-2380 μm size in *κ*-carrageenan hydrogel matrix enabled to increase the oral residence time. On the other hand, Tang, et al. (2016) showed the impact of using textural heterogeneity with seeds as well as layering arrangements within gelatin-agar hydrogels on increasing satiation. Temporal perception of texture contrast was recently investigated by Santagiuliana, et al. (2018), where authors employed layering approaches to generate mechanical contrast in agar, *κ*-carrageenan, and gelatine hydrogels and suggested that a combined effect of mechanical and

physicochemical properties influenced the dynamic perception of inhomogeneity over time. Nevertheless, to our knowledge, creation of hydrogels with systematic manipulation of structural complexity and understanding the impact of those manipulations on 'chewing-' and 'lubrication-' related texture attributes that are perceived during early and later stages of oral processing, respectively, have not been investigated to date.

The aim of this study was to understand the relationship between rheological, tribological and sensory properties (n=11 panellists) of hydrogels differing in hydrocolloid type, concentration and degree of inhomogeneity. Our hypothesis was that initial fracture properties of the hydrogels and apparent viscosities of the gel boli could be correlated with chewing-related texture attributes, whereas tribological properties (i.e. friction coefficients in boundary and mixed lubrication) of the gel boli could be correlated with lubrication-related texture attributes. A range of hydrogels using *κ*-carrageenan, locust bean gum (LBG), sodium alginate and calcium alginate with different degrees of structural complexity and inhomogeneity were employed to test this hypothesis.

κ-Carrageenan forms a tight-knit molecular network that results in the formation of a strong homogenous gel matrix. Since real food is not homogeneous, a degree of structural complexity was achieved in the samples by manipulating *κ*-carrageenan gels using LBG or sodium alginate to form mixed gels. Incorporation of LBG can strengthen *κ*-carrageenan's continuous network, promoting elastic properties and reducing syneresis. This synergistic interaction is attributed to the ability of LBG to form stable cross-links with *κ*-carrageenan (Stading & Hermansson, 1993). On the other hand, sodium alginate is known to interfere with the incipient coil-to-helix transition during the formation of the *κ*-carrageenan gel, and thus the sodium alginate + *κ*-carrageenan mixture is expected to create a weaker mixed gel (Laguna & Sarkar, 2016). To add another dimension to the structural complexity, a level of inhomogeneity was introduced in the *κ*-carrageenan gels by inclusion of calcium alginate beads of different

particle sizes, where the latter behaved as “inactive filler particles” (Laguna & Sarkar, 2016). Presence of calcium alginate beads would likely lead to a decrease of mechanical strength due to interruption of the continuous *κ*-carrageenan network by these beads that acted as structural defects. To our knowledge, this is the first study that attempts to examine the relationship between rheology, tribology and sensory perception in hydrogels and findings from this study should provide useful information for the design of novel foods with specifically tailored oral texture and sensory properties.

2. Materials and methods

2.1. Materials

Food grade quality kappa-carrageenan, locust bean gum and sodium alginate were purchased from Special Ingredients Ltd (Chesterfield, UK). Green food colouring was obtained from AmeriColor (Placentia, USA) and American peppermint extract was purchased at a local supermarket (Leeds, UK). Potassium chloride was purchased from Minerals Water Ltd (Purfleet, UK) and calcium chloride from VWR International (Leuven, Belgium). Additionally, sodium chloride, potassium phosphate, potassium citrate, uric acid sodium salt, urea, lactic acid sodium salt, and porcine gastric Mucin Type II were obtained from Sigma-Aldrich (St. Louis, USA). All materials were used without further purification. Demineralised water was used in preparation for all the gels and the artificial saliva formulation.

2.2. Preparation of the hydrogels

The composition of the hydrogels is shown in **Table 1**. Visual images of the seven hydrogels are shown in **Supplementary Figure 1**. Typically 400 g of sample was prepared and poured into petri-dishes to a height of 2 cm (150 g gel per petri-dish), and then kept overnight at 4 °C.

Cylindrical pieces of the hydrogels were cut out from the petri-dish using a circular cookie cutter (diameter 25 mm, height 10 mm), and used as such for all measurements.

2.2.1. Kappa-carrageenan hydrogels

For preparation of kappa-carrageenan hydrogels (κC), appropriate quantities of κC were dispersed in a 0.2 M potassium chloride (KCl) solution and stirred for 30 min to ensure maximum hydration. Then, the solution was heated up in a shaking water bath at 98 °C for 1 h. The gelling solutions were allowed to cool down for 5 min, and finally the green colouring and peppermint flavouring were added before being allowed to set in petri-dishes.

2.2.1. Kappa-carrageenan/ LBG or kappa-carrageenan/sodium alginate hydrogels

The mixed hydrogels were prepared by mixing the appropriate quantities of powdered κC and LBG or sodium alginate (NaA) together before adding the respective powder mixtures to distilled water and mixing for 30 min. Then, the solutions were heated up in a shaking water bath at 98 °C for 1 h. The solutions were allowed to cool down for 5 min, and finally the green colouring and peppermint flavouring were added before being allowed to set in petri-dishes.

2.2.2. Kappa-carrageenan/calcium alginate hydrogels

The calcium alginate (CaA) beads were prepared first and then added as a layer in the κC hydrogels (before the gels were allowed to set) to create a level of inhomogeneity within the gels, based on a previous study (Laguna & Sarkar, 2016). The beads were prepared by making a 1 wt% NaA solution in water, and stirring for 1 h to ensure complete hydration. Calcium chloride ($CaCl_2$) solutions of 0.01 M and 0.05 M were prepared to make the 300 μm and 1000 μm sized beads, respectively. The 1 wt% NaA solution was passed through a Buchi Encapsulator B-390® (Buchi UK Ltd, Chadderton, UK) with a vibrating nozzle and then

dropped into the appropriate $CaCl_2$ solutions while being stirred to create the CaA beads. A vibrating nozzle of 300 μm (frequency 500 Hz, air pressure 250 mbar) or 1000 μm (frequency 700 Hz, air pressure 300 mbar) was used depending on the required bead size. The beads were allowed to set in the $CaCl_2$ solution at room temperature for 30 min under constant stirring. The beads were subsequently washed thrice with distilled water and then air-dried. Meanwhile, the κC solution was prepared by dissolving the appropriate amount in distilled water and mixing for 30 min. Then, the solution was heated up in a shaking water bath at 98 °C for 1 h and allowed to cool down for 5 min followed by adding the green colouring and peppermint flavouring. The appropriate amount of CaA beads was weighed and added to the petri-dish and the κC gels solution was poured, before allowing the gel to set similar to the preparation method of the aforementioned hydrogels.

2.3. Texture analysis

Uniaxial single compression tests were carried out using a TA-TX2 Texture Analyzer (Stable Micro Systems Ltd., Surrey, UK), attached with a 50 kg load cell. In the compression test, the samples were compressed using a cylindrical probe (diameter 59 mm). The tests were carried out at 22 °C, at a constant speed of 2 mm/sec and the deformation level was set at 80 % strain. At least three repeats were recorded for each gel on at least four different gel preparation days. The software Exponent (TEE32, v6.1.9.0, Stable Micro Systems Ltd., Surrey, UK) was used to obtain the force-distance curves, and the fracture mechanics were calculated from these curves. The fracture properties were determined at the maximum point of the stress-strain curves. The fracture energy was determined as the area under the curve up to the fracture point (Peleg, 1984). The initial slope of all samples was determined up to a stress of 500 Pa, as this was considered within the viscoelastic limit.

2.4. Preparation of artificial saliva

Artificial saliva was prepared according to the method previously described by Sarkar, et al. (2009). Briefly, artificial saliva was composed of 0.16 g/L NaCl, 0.33 g/L NH_4NO_3, 0.64 g/L K_2HPO_4, 0.2 g/ L KCl, 0.31 g/L $K_3C_6H_5O_7.H_2O$, 0.02 g/L $C_5H_3N_4O_3Na$, 0.2 g/L H_2NCONH_2, 0.15 g/ L $C_3H_5O_3Na$ and 3 g/L mucin. The pH of the saliva solution was adjusted to pH 6.8 using 1 M NaOH. Noteworthy, porcine mucin was used in the artificial saliva to simulate the human salivary viscosity at comparable concentrations present in human saliva. However, bovine submaxilliary mucin could be a promising alternative considering its ability to form more elastic films and its higher lubricating properties particularly in elastomeric contact surfaces (Madsen, et al., 2016).

2.5. Simulated oral processing

The hydrogels were broken down mechanically in the presence of artificial saliva to mimic oral processing. The samples were put into a mechanical blender (Andrew James UK Ltd, Bowburn, UK) with artificial saliva in a ratio 2:1 w/w and homogenized for 15 seconds at low speed (speed 1). Depending on the hydrogel tested, the obtained particle size was < 2-5 mm. After grinding, the gel was mixed with artificial saliva (final sample to saliva ratio 4:3 w/w) and left to rest for 30 min. It is worth highlighting that the amount of saliva incorporated in the food bolus has varied across studies from as low as 8 wt% saliva in vivo in emulsion gels (Devezeaux de Lavergne, van de Velde, van Boekel, & Stieger, 2015a) to 18 wt% artificial saliva incorporation in vitro to create model hydrogel boli (Ishihara, Nakauma, Funami, Odake, & Nishinari, 2011) to 50 wt% simulated saliva addition for food matrices in case of harmonized INFOGEST static model (Minekus, et al., 2014). For our study, we used a ratio of 4:3 (w/w) sample:saliva to have the same level of saliva incorporation across all samples to enable comparison, though we highlight the limitation that during oral processing (in vivo), the amount

of saliva added to the samples would not be the same across the different hydrogels with varying degrees of complexity.

The broken down hydrogel:saliva mixture samples, from here on defined as 'gel bolus fragments', were used for the rheological and tribological measurements. To understand the thin-film properties, the tribological properties were also measured for the samples where any large gel particles (> 500 µm) were filtered out, from here on defined as 'gel bolus filtrate'.

2.6. Apparent viscosity

The apparent viscosities of the gel fragments in presence of artificial saliva were measured using a rheometer (Kinexus Ultra+, Malvern Instruments Ltd, Worcestershire, UK) equipped with a plate-plate geometry (diameter 60 mm). The gap size (ranging from 0.01-0.15 mm) was individually adjusted for each gel, depending on their particle size once broken down. To prevent evaporation, the samples were sealed off with a thin layer of silicone oil. Flow curves were obtained for all gel samples after simulated oral processing at shear rates ranging from 0.0001 to 100 s^{-1} at 37 °C. A minimum of three measurements were performed for each sample. Associated Ostwald de Waele power law (equation (1) was fitted to the viscosity of each sample:

$$\eta = K\dot{\gamma}^{n-1} \quad (1)$$

where η is the apparent viscosity, K is the consistency index (Pa s) and n is the behaviour index. These parameters were utilised in the determination and validation of the corresponding viscosities calculated by entrainment speeds and permitted friction coefficients to be plotted against the entrainment speed and viscosity products as described in the tribology section.

It is noteworthy that detailed rheological characterization of the viscoelasticity of the hydrogels and the corresponding bolus fragments was not carried out in this study.

2.7. Oral tribology

The oral tribological properties of the gel bolus fragments and gel bolus filtrates were determined using a ball-on-disc set up in a Mini Traction Machine (MTM2, PCS Instruments, London, UK). The gel bolus samples were prepared according to the method described above. Commercially available polydimethylsiloxane (PDMS) ball (diameter of 19 mm, MTM ball Slygard 184, 50 Duro, PCS Instruments, London, UK) and disc (diameter of 46 mm, thickness of 4 mm, MTM disc Slygard 184, 50 Duro, PCS Instruments, London, UK) were used for the measurements (surface roughness of PDMS tribopairs, R_a < 50 nm). The PDMS surface contacts were kept a minimum of 2 h submerged in artificial saliva to create a mucin film with the intent to simulate the oral conditions. The sample was loaded into the pot equipped with the PDMS disc; the ball was lowered onto the disc and then the pot was covered with a lid. The PDMS ball and disc were rotated at different speeds to create a relative motion between the surface of the ball and the disc, resulting in a slide-to-roll ratio (SRR) of 50%, to impart both rolling and sliding motions (Sarkar, et al., 2017a) and the temperature was maintained at 37 °C, simulating oral conditions.

Two parameters have been used for both the ball speed and the disc speed: one with $V_{ball} > V_{disc}$ and one with $V_{ball} < V_{disc}$, while keeping the SRR constant. The entrainment speed was calculated as the average of the two measures to remove any offset errors in the lateral force measurement, as well to remove any friction that did not reverse sign when the speeds were reversed, such as rolling friction (Bongaerts, Fourtouni, & Stokes, 2007a). Thus, the entrainment speed was defined as:

$$\bar{U} = \frac{1}{2}(U_1 + U_2) \quad (2)$$

where U is the entrainment speed and U_1 and U_2 are the velocities of the two contacting surfaces (i.e. ball and disc). The rolling speed was reduced from 1000 to 1 mm/s and friction forces were measured to obtain a Stribeck curve. All tests were performed at a load of 2 N, as this is a good representative value of loads occurring in the mouth while maintaining sensitivity in the tribometer. Average and standard deviation were calculated from three measurements on replicate samples. Following the studies by de Vicente, StokesSpikes (2005) and Bongaerts, et al. (2007a), we utilized the Stribeck 'master curve' (equation 3) to enable comparison of sample friction coefficient μ against the product of entrainment velocity U and sample viscosity η:

$$\mu_{total} = \mu_{EHL} + \left(\frac{\mu_b - \mu_{EHL}}{1 + \left({}^{U\eta}/_{B}\right)^{m}}\right) \quad (3)$$

where

$$\mu_{EHL} = k(U\eta)^n \quad (4)$$

and

$$\mu_b = h(U\eta)^l \quad (5)$$

where, (k, n) and (h, l) are the elastohydrodynamic lubrication (EHL) and boundary layer power law coefficient and index respectively. Here, B relates to the threshold value of $U\eta$ for boundary friction and m represents the mixed regime exponent. It is worth pointing out that the flow

curves (in the above section) were only determined for gel fragments to relate to the early stages of oral processing where bulk properties tend to dominate. However, friction coefficients were determined for both bolus fragments and filtrates, latter resemble the thin layer formed between the contact surfaces (e.g. tongue and palate) in later stages of oral processing, where surface properties dominate (Chen & Stokes, 2012; Laguna & Sarkar, 2017; Stokes, et al., 2013).

2.8. Descriptive sensory analysis

A panel was recruited from the University of Leeds to participate in a descriptive sensory analysis. The panel was selected and familiarized with the hydrogel samples followed by generation of attributes and introduction to the used rating scale. The study was reviewed and approved by the Faculty Research Ethics Committee at the University of Leeds (ethics reference MEEC 16-006). A group of 11 participants (4 male, mean (± SD) age = 28.8 (± 5.5) years, range 21-40 years) was trained to familiarize them with the different hydrogel samples and to create a list of relevant attributes related to the chewing as well as the lubrication aspects of the gels.

Three training sessions of 1 h each were conducted with the seven hydrogel samples. During the first training session, the hydrogels were tasted to familiarise the participants with the type of samples, and participants were encouraged to come up with terms to describe the different texture aspects of the different gels. Subsequently, an extensive list of potential attributes related to both the chewing and lubrication aspects was introduced to the participants and their applicability and definitions were discussed in the group. During the second session, the list of attributes generated during the first training session was further specified to describe the difference between the textural aspects of the gels as best as possible and to reach a consensus within the panel. Finally, in the last training session the rating scales were introduced

and a group discussion resolved how to use the scales for the different attributes in the included samples and the best order in which to rate these attributes.

After completion of the training, the samples were evaluated in individual sensory test booths under normal lighting conditions, with the samples presented in randomised order in triplicate in a balanced block design divided over two test days (with 11 samples rated on day one and 10 samples on day two). All samples were prepared 24 h prior to the sensory assessment, presented in individual cups labelled with a three-digit code, and moved to room temperature 20 min before the start of the test. A practice sample was provided on each test day to get a sense of the samples before the start of the test due to the novelty of these hydrogels. As determined by the training sessions, nine different texture attributes were rated for each sample in a fixed order (see **Table 2**).

The intensities of the different attributes were rated onto an unstructured line scale of 100 mm, as presented with the software CompuSense (v5.0, Ontario, Canada), anchored from 'not at all' (0) to 'very' (100). All panellists followed the same tasting procedure, putting the sample as a whole in the mouth. It was optional for the panellists to choose whether to swallow the sample at the end or spit it out in provided cups. Between each sample, panellists were instructed to rinse their mouth with water and eat a cracker to cleanse their palate. Data was extracted from the software and exported to SPSS (IBM® SPSS® Statistics, v24, SPSS Inc, Chicago, USA) for analysis.

2.9. Statistical analysis

Mean values and standard deviations (SD) were calculated using Excel (Microsoft Office 2010). For each sample, sensory attribute and assessor in the sensory analysis, the panel performance was checked to make sure there were no clear outliers or obvious errors using the software PanelCheck (v1.4.2). The panel performance was assessed and panel agreement,

discrimination and repeatability among assessors was considered to be acceptable according to the Tucker-1, F- and MSE-plots, respectively (Tomic, et al., 2010), and thus, no data was removed.

In addition, Principal Component Analysis (PCA) was conducted on the nine sensory attributes with orthogonal rotation (Direct Oblimin). The Kaiser-Meyer-Olkin measure verified the sampling adequacy for the analysis: KMO = 0.788, which is well above the acceptable limit of 0.5 (Field, 2017). Bartlett's test of sphericity χ^2 (36) = 1197.985, $p < .001$, indicated that correlations between items were sufficiently large for PCA. An initial analysis was run to obtain eigenvalues for each component in the data. Two components had Eigenvalues over Kaiser's criterion of 1 and in combination explained 64.1% of the variance, and thus were retained in the final analysis.

In order to study the differences in samples for all selected attributes, analysis of variance (one-way ANOVA) was applied to the ratings data from the sensory panel with the samples as fixed factor; least significant differences were calculated by Bonferroni's post-hoc test. Similarly, differences between samples for the mechanical analyses (uniaxial compression test of hydrogels, flow curves of bolus fragments, friction coefficients of gel bolus fragments and filtrates) were determined with one-way ANOVA and Bonferroni post-hoc testing. Pearson's product moment correlations were calculated to assess the simple relationships between the different instrumental and sensory characteristics of the hydrogels. All statistical analyses were performed in SPSS (IBM® SPSS® Statistics, v24, SPSS Inc, Chicago, USA), and statistical significance level was set at $p < 0.05$.

3. Results and discussion

3.1. Mechanical characterisation of hydrogels and simulated boli

3.1.1. Texture analysis of the hydrogels

The fracture stress and strain of the seven hydrogels are shown in **Figure 1**. The samples can be categorized into three groups: 1) high fracture stress/high fracture strain, 2) intermediate fracture stress/fracture strain, and 3) low fracture stress/low fracture strain. Group 1 included the two *κ*C samples (2 wt% and 3 wt%) and the *κ*C/LBG sample, averaging a fracture stress of 190 kPa and a fracture strain of 1.17. Group 2 included the samples containing the CaA beads, with an average fracture stress and fracture strain of 71 kPa and 0.93, respectively, where the particle size of CaA beads (300 or 1000 µm) did not show any significant contribution to the fracture mechanics at equivalent biopolymer concentration ($p > 0.05$). Group 3 consisted of the *κ*C/NaA hydrogels with an average fracture stress of 27 kPa and a fracture strain of 0.70. The high and low fracture stress samples varied by a factor 7 and the samples in the low and high fracture strain groups varied by a factor 1.8. The fracture energy of the hydrogels, shown in **Supplementary Table 1**, also indicate that the samples were categorized in similar groups as in **Figure 1**. Based on these groupings, **Figure 2** shows a schematic representation of the structures of these hydrogels.

As expected, the fracture stress followed a power law increase with increased concentration of *κ*C in native *κ*C hydrogels (**Figure 1**), allowing the formation of a three-dimensional network structure (as shown schematically in **Figure 2**) induced by the supramolecular aggregation of the double helices (Laguna & Sarkar, 2016). Interestingly, the fracture stress of the 2.25*κ*C0.75LBG hydrogel was significantly lower than that of 3*κ*C hydrogel at equivalent total biopolymer concentration ($p < 0.05$). This is not in line with previous findings, where it has been reported that LBG has the ability to strengthen the *κ*C network by forming multiple junction zones between LBG un-substituted mannan backbones

and κC helices (Dea & Morrison, 1975; Devezeaux de Lavergne, Strijbosch, Van den Broek, Van de Velde, & Stieger, 2016; Dunstan, et al., 2001). A possible explanation for this could be the difference in total biopolymer concentrations and the ratio between κC and LBG used in this study versus previous reports. Interestingly, Czaczyk, OlejnikTrojanowska (1999) also observed similar weakening effect of LBG on κC hydrogels at 2-3 wt% total biopolymer concentration in a ratio of κC: LBG of 2:1 w/w i.e. similar to the range used in this study.

Unsurprisingly, the presence of NaA (1.5κC0.5NaA hydrogel) resulted in significant weakening of the κC gel (**Figure 1**), which might be attributed to the segregative interaction between NaA and κC, disrupting the coil-to-helix transition during κC hydrogel formation (**Figure 2**), finally leading to a phase separated κC/NaA hydrogel (Goh, Sarkar, & Singh, 2008, 2014; Laguna & Sarkar, 2016). On the other hand, the presence of CaA beads (1.6κC0.2CaA_{300}, 1.6κC0.2CaA_{1000}) contributed to considerable reinforcement of the κC hydrogel as compared to that of the presence of NaA (1.5κC0.5NaA). Introducing defects due to the presence of these CaA beads as "inactive filler particles", resulted in a less defined network (**Figure 2**) with less fracture stress as compared to that of a native κC hydrogel (**Figure 1**). Based on the texture analysis results, it can be concluded that the chosen hydrogel types covered a wide range of deformation behaviour, which can be hypothesized to have different sensory properties, particularly in terms of chewing-related attributes.

3.1.2. Apparent viscosity of the hydrogel bolus

Figure 3 shows the apparent viscosity (η) of the bolus particles derived from simulated oral processing of the hydrogels in the presence of artificial saliva at 37 °C. All bolus fragments in presence of artificial saliva showed extreme shear thinning behaviour, with slight indications of plateau values being reached only at low shear rate limits (10^{-3} s^{-1}). Such pseudoplastic

behaviour is in agreement with that of protein-based microgels, where latter showed similar ranges of η values as a function of volume fraction and shear rate (Sarkar, et al., 2017a).

In addition, high values of η persisted in boli of both κC hydrogels and mixed hydrogels even after subjection to fairly high i.e. orally relevant shear of 50 s^{-1}. As expected, due to the aforementioned segregative interaction between κC and NaA, the bolus of 1.5κC0.5NaA hydrogels were one to two orders of magnitude lower in η as compared to that of the rest of the hydrogels (κC, κC/LBG and κC/CaA) even though all the systems were highly shear thinning. It is worth noting that at oral shear (50 s^{-1}), η of 1.5κC0.5NaA hydrogel bolus fragments and the rest of the (κC, κC/LBG and κC/CaA) hydrogel bolus fragments was three or four orders of magnitude higher than artificial saliva (**Figure 3**) or real human saliva, respectively (Bongaerts, Rossetti, & Stokes, 2007b). This suggest that the rheology might play an important role in driving the load bearing capacity of these gel bolus fragments during oral tribology experiments and consequently sensory perception. However, viscosity results might not be sufficient to understand the underlying mechanism of differences in the friction coefficients (if any) between κC, κC/LBG and κC/CaA hydrogel bolus, as the viscosities were not significantly different between these gel bolus fragments at orally relevant shear rates ($p > 0.05$). Furthermore, one might investigate how the viscoelastic parameters of the bolus fragments may impact the load bearing aspects and oral processing attributes, which is beyond the scope of this study and needs to be studied in future.

3.1.3. Oral tribology of the hydrogel bolus fragments and filtrates

It is well recognized that the rheological properties (bulk phase) dominate the textural sensation only in the early stages of oral processing. It is now postulated that oral tribology (surface properties) dictates the thin-film properties and thus the oral sensation in the later stages of oral processing where the food and/or food-saliva mixture interact with the oral surfaces (Chen &

Stokes, 2012; Laguna & Sarkar, 2017; Pradal & Stokes, 2016; Stokes, et al., 2013). To understand this surface phenomenon, the coefficient of friction (μ) of both gel bolus fragments and gel bolus filtrate (i.e. the thin-film) when sheared between smooth hydrophobic PDMS-PDMS ball and disc tribopairs was plotted as a function of entrainment speed as shown in **Figures 4a** and **4b**, respectively. Although attempts were made to pre-adsorb artificial salivary films to hydrophobic PDMS substrates, there was no change in the water contact angle (θ) of the substrates (data not shown) and the PDMS surface remained hydrophobic (θ = 108 °) as studied previously (Sarkar, et al., 2017a; Yakubov, McColl, Bongaerts, & Ramsden, 2009).

The plateau boundary ($\bar{U} \leq 10$ mm/s) and mixed regimes ($10 < \bar{U} \leq 300$ mm/s) of lubrication could be clearly identified in the Stribeck curves of the measured samples (**Figures 4a** and **4b)**. Considering the relevance of biologically relevant speeds, such as the speed of the human tongue being ~ 20 mm/s (Steele & Van Lieshout, 2009), we have focussed only on boundary and mixed lubrication regimes. The artificial saliva, which served as a control, showed a classical Stribeck profile with μ varying from 0.3–0.5 in the boundary regime, falling off by one-order of magnitude in the mixed regime. This is consistent with ranges of values found in a previous study using the same artificial saliva formulation (Laguna, et al., 2017a).

In the boundary conditions, the PDMS ball and disc appeared to be in near-adhesive PDMS-PDMS (intimate) contact, where the entrainment of the hydrogel bolus fragments or filtrates was rather poor (**Figures 4a** and **4b)**. Interestingly, gel fragments containing higher concentration of *κ*C (3*κ*C), LBG (2.25*κ*C0.75LBG) and alginates as beads (1.6*κ*C0.2CaA$_{1000}$, 1.6*κ*C0.2CaA$_{300}$, 2.4*κ*C0.2CaA$_{300}$) showed some sort of entrainment even in the boundary regime reducing the friction force significantly (< 0.4 N) as compared to that of artificial saliva ($p < 0.05$) (**Table 3**). Gong & Osada (1998) described a "repulsion–adsorption model" to explain friction in hydrogels, which suggests that the friction force is the sum of elastic force and vicious force, which can be applied to these gel bolus fragments. The elastic force arises

from anchorage of the biopolymer to the substrate (adhesive), whereas the viscous force results from the hydration of the polymer (repulsive) (Gong & Osada, 1998; Gong, 2006; Stokes, Macakova, Chojnicka-Paszun, de Kruif, & de Jongh, 2011). At a first glance, it seems that the reduction in μ in the boundary regime of these gel fragments (3κC, 2.25κC0.75LBG, 1.6κC0.2CaA$_{1000}$, 1.6κC0.2CaA$_{300}$, 2.4κC0.2CaA$_{300}$) might be associated with interactions between κC, LBG, NaA or CaA hydrogels and the PDMS substrates allowing biopolymer adsorption to some degree. However, this is somewhat unlikely considering the high hydrophobicity of PDMS (Sarkar, et al., 2017a) and hydrophillicity of these gels.

Hence, the relevance of 'opposing substrate' in friction in this case is worth recognizing (Gong, Kagata, Iwasaki, & Osada, 2001). Note, both κ-carrageenan and alginates are highly negatively-charged biopolymers at pH 6.8. Thus, repulsions from both opposing PDMS substrates (artificial saliva coated i.e. negatively charged) (Sarkar, et al., 2009; Sarkar, et al., 2017a) as well as the opposing gel surfaces (i.e. inter-gel repulsion between negatively-charged gel bolus fragments) (Bongaerts, Cooper-White, & Stokes, 2009; Gong, Kagata, & Osada, 1999; Gong & Osada, 2002) are highly likely. Such repulsive interactions against the opposing artificial saliva coated PDMS substrate and/or the gel fragment surfaces, might have enabled these hydrogel fragments to remain hydrated forming a thicker solvent layer of 'lubricant', thus providing an effective barrier to the asperity contacts under the low load. This is further justified by the high viscosity values of these specific gel fragments (**Figure 3)** suggesting viscous force as the driving factor and separating the PDMS contacts effectively (**Figure 4a**).

As the sliding speed of the disc started to increase, μ decreased in all samples (**Figures 4a and Figures 4b**) and started to fill the gap between the surface asperities of the tribopairs in the mixed lubrication regime. The inclusion or exclusion of gel fragments or gel filtrate largely depends on the gap between the contacting surfaces, the size of the gel fragments compared to the size of the gap and asperities, as well as the interactions of these gel fragments

with the PDMS surfaces. In the case of gel bolus fragments containing beads (1.6κC0.2CaA$_{1000}$, 1.6κC0.2CaA$_{300}$, 2.4κC0.2CaA$_{300}$) (**Figure 4a**), the μ was one-order of magnitude lower than artificial saliva ($p < 0.05$). The beads were larger in size as compared to the asperities of the PDMS substrates (R_a = 50 nm) and thus the beads released from the gel fragments during simulated oral processing might have rolled into the contact zone between the PDMS tribopairs, thus reducing μ values. It is tempting to propose a "ball-bearing mechanism" for the reduction in μ using CaA, such mechanism has been previously postulated for whey protein particles and protein microgel particles (Liu, Tian, Stieger, van der Linden, & van de Velde, 2016; Sarkar, et al., 2017a).

To test the possibility of this ball-bearing mechanism occurrence, the Hertz pressure effects for the CaA beads of 1000 and 300 μm were calculated with the assumption that 10% of the beads were entrained between the PDMS ball and disc surfaces (de Vicente, et al., 2005; Johnson, 2009; Johnston, McCluskey, Tan, & Tracey, 2014; Puttock & Thwaite, 1969). The Young's modulus for CaA beads was assumed to be 20 kPa, based on previous studies (Larsen, Bjørnstad, Pettersen, Tønnesen, & Melvik, 2015). From Hertz theory, the spherical contact area of the PDMS ball and disc was calculated using Eq (3):

$$\pi\alpha^2 = 1.31\left(\frac{R'F}{E'}\right)^{0.67} \quad (3)$$

where, α is the surface contact, R' is the reduced radius of the PDMS ball, F is the force for each particle entrained between the two contacts and E' is the reduced elastic modulus. The E' was defined as:

$$\frac{2}{E'} = \frac{1-\sigma_1{}^2}{E_1} + \frac{1-\sigma_2{}^2}{E_2} \quad (4)$$

where, σ is the Poisson's ratio, assumed to be 0.5, and E is the Young's modulus (de Vicente, et al., 2005).

The number of particles in the contact area was calculated as:

$$N_{particles} = \frac{\varphi_{particles} \times A}{\pi R^2} \quad (5)$$

with φ being the concentration of particles in the contact zone, A the area of contact ($\pi\alpha^2$) and R the radius of the particles. Hence, the force per particle was calculated as:

$$F_{particle} = \frac{F_{total}}{N_{particles}} \quad (6)$$

with F the total force applied and N the number of particles. Finally, the spherical contact area was determined using the approach of distant points (Johnson, 2009):

$$\alpha = \left(\frac{9F^2}{16R'E'^2}\right)^{1/3} \quad (7)$$

with *E'* defined as:

$$E' = 2\left(\frac{1-{\sigma_1}^2}{E_1} + \frac{1-{\sigma_2}^2}{E_2}\right)^{-1} \quad (8)$$

The results shown in **Table 4** clearly indicate that the CaA particles were not capable of rolling as α >> size of the beads, even with 10% particles being entrained between the PDMS surfaces. Interestingly, the 1000 µm CaA beads were too large to actually be entrained in the contact zone. These calculations indicate that there was no "ball-bearing effects" using CaA

irrespective of the particle size studied, and the reduction in μ could be explained by the rheological behaviour (**Figure 3**) of the gel boli containing beads forming the viscous layer as the 'lubricant', as discussed previously. Also, not to underestimate, that the amount of water within these gel beads might also play an important role in exhibiting low friction (Gong & Osada, 2002). The water might be squeezed out the gel beads forming a thin-film and may serve as a 'boundary lubricant'.

In case of the gel filtrates (**Figure 4b**), the Stribeck curve of the *κ*C hydrogels almost overlapped irrespective of the biopolymer concentration in both boundary and mixed lubrication regimes ($p > 0.05$). Similarity in friction forces for both 2*κ*C and 3*κ*C hydrogel bolus filtrates and artificial saliva irrespective of entrainment speeds (**Table 3**) suggests that the hydrogel bolus filtrates lacked the ability to migrate into and replenish the confined region in the event that the two PDMS shearing surfaces were almost in direct contact. This is unlike the behaviour in **Figure 4a**, where *κ*C gel bolus fragments showed entrainment driven by the viscosity of the hydration layer created by the gel bolus fragments (**Figure 3**). As expected, such influence of rheology on tribology was not evident in the hydrogel bolus filtrates owing to the loss of the gel fragments particles during filtration (**Figure 4b**). In the mixed lubrication regime, the filtrates from hydrogel boli containing LBG (2.25*κ*C0.75LBG), NaA (1.5*κ*C0.5NaA) or CaA (1.6*κ*C0.2CaA$_{1000}$, 1.6*κ*C0.2CaA$_{300}$, 2.4*κ*C0.2CaA$_{300}$) contributed to significantly lower friction forces as compared to the artificial saliva ($p < 0.05$) (**Table 3)**. This complies with the behaviour observed for the corresponding hydrogel bolus fragments (**Figure 4a**). Even after filtration, the spherical CaA beads might have been retained in the filtrate enabling some degree of entrainment (**Table 4**), or both gel fragments containing NaA and CaA were increasing the lubrication effect, possibly by 'weeping out' the water layer as a thin-film 'boundary lubricant' (Gong & Osada, 2002).

In our study, the fitted values with the Stribeck master curve i.e. k = 0.0065, n = 0.55, h = 11, l = 0.075, B = $0.33 \cdot 10^{-4}$, m = 1.0 gave a good fit (Bongaerts, et al., 2007a; de Vicente, et al., 2005). Here it should be noted that since the samples were shear thinning (**Figure 3**), the viscosity multipliers were calculated at each entrainment velocity. This was achieved by fitting the entrainment speeds to the shear rate by use of a power law relation of the same format as Eq (7), and which enabled calculation of the associated viscosity. In this study, entrainment speeds of 1 to 1000 mm/s translated to shear rates of 0.1 - 100 s^{-1}. This was validated to ensure the entrainment speeds did indeed coincide with shear rates and that the predicted viscosities agreed with the shear rate/viscosity Ostwald de Waele power law regressions relevant to each sample.

As can be seen in the master curve (**Figure 5**), good agreement was achieved in the mixed regime and from the transitionary region into the EHL. However, in contrast to Newtonian lubricants (Bongaerts, et al., 2007a; de Vicente, et al., 2005), using the particulate hydrogel bolus fragments, the model failed in the boundary regime. This suggests that the hydrogel bolus particles had a different degree of entrainment in the boundary regime and the key mechanism of friction reduction in the boundary regime was due to opposing surface-mediated formation of a viscous layer of 'gel fragments' (**Figure 4b**). As one might expect, such layer formation varied as a function of sample inhomogeneity under shear conditions in confinement and samples with inhomogeneity indicated a limitation in the Stribeck representation in this regime.

3.2. Descriptive sensory analysis of the hydrogels

Table 2 summarizes the sensory attributes generated by the sensory panel together with their definitions. Nine different texture attributes were selected that were perceived during oral processing of the hydrogels. With the first two principal components (PC), 64% of the variance

585 in the data was explained and the PCA plot showed that attributes were clustered in three groups
586 (**Figure 6**). The pattern matrix, **Table 5**, shows that PC1 included the attributes related to the
587 chewing aspects: 'firm', 'elastic', 'chewy' and 'cohesive', as well as the inverse of the
588 attributes more related to lubrication: 'pasty' and 'melting'. The PC2 was represented by
589 attributes that could be considered in the oral lubrication domain: 'smooth', 'slippery' and
590 'salivating'. At first bite, perceived firmness of a solid or semi-solid food is known to be related
591 often to the fracture stress (Foegeding, et al., 2011). In fact, in this study, for all the chewing-
592 related attributes (see **Figure 7**), the hydrogels could be categorised into two key groups. Group
593 1) included the hydrogels with high fracture stress/high fracture strain (*κ*C and *κ*C/LBG gels)
594 (**Figure 1**) that generally scored high on the chewing-related texture attributes, such as 'firm',
595 'elastic' and 'cohesive', and Group 2) included the hydrogels with low fracture stress/low
596 fracture strain (*κ*C/NaA and *κ*C/CaA gels) that scored low on these attributes. As one might
597 expect, the chewing-related texture attributes were strongly dominated by the concentration of
598 *κ*C i.e. higher concentration of *κ*C (3wt%) resulted in more 'firm' and 'chewy' perception as
599 compared to that created using lower concentrations (2 wt%) ($p < 0.05$). Similarly for samples
600 containing beads of the same size (300 µm), a higher concentration of *κ*C (2.4 wt%) resulted
601 in creating samples ($2.4\kappa C0.2CaA_{300}$) that scored on the higher end of the 100 mm scale and
602 were more 'firm', chewy', 'elastic' and 'cohesive', as compared to that created using lower *κ*C
603 concentrations (1.6 wt%) ($p < 0.05$) . Although the presence of beads and their particle size
604 (300 versus 1000 µm) significantly influenced the fracture mechanics during the uniaxial
605 compression test (**Figure 1**), this was not apparent in the sensory analysis of the four chewing-
606 related texture attributes ($p > 0.05$) (**Figure 7**).
607 The lubrication-related texture attributes (see **Figure 8**) appeared to show a somewhat
608 opposite effect, with the low fracture stress/low fracture strain samples scoring high on
609 'melting' and 'pasty', whereas the high fracture stress/high fracture strain samples scored

610 relatively low on the 100 mm scale. The *κ*C/NaA hydrogel (1.5*κ*C0.5NaA) scored high on most
611 of the lubrication-related texture attributes, such as 'smooth', 'pasty', 'melting'. It is worth
612 remembering that the 1.5*κ*C0.5NaA hydrogel bolus had the lowest η (though three-orders of
613 magnitude higher than human saliva) as compared to the other samples (**Figure 3**).
614 Nevertheless, the higher scores on the lubrication-related texture attributes of the *κ*C/NaA
615 hydrogel is in close agreement with the lower μ values (**Figure 4b**), and correspondingly lower
616 friction force in both boundary and mixed lubrication regimes for the hydrogel bolus filtrate
617 (**Table 3**). This suggests that the viscosity-parameter could not explain the lubrication-related
618 texture attributes in case of *κ*C/NaA hydrogel and it was the 'weeping' water film that might
619 have acted as a 'boundary lubricant'. Interestingly, the *κ*C and *κ*C/LBG hydrogels scored
620 significantly low on 'pasty' and 'melting' ($p < 0.05$), congruent with the high μ of the hydrogel
621 bolus filtrate (**Figure 4b**) and their correspondingly high friction forces in both the boundary
622 and mixed regimes (**Table 3**).

623 The *κ*C/CaA hydrogels with beads (1.6*κ*C0.2CaA$_{300}$, 1.6*κ*C0.2CaA$_{1000}$,
624 2.4*κ*C0.2CaA$_{300}$) scored rather intermediate (30-60 mm) on all lubrication attributes. They
625 were perceived to be more 'melting' and 'pasty' as compared to the *κ*C and *κ*C/LBG hydrogels
626 ($p < 0.05$) (**Figure 8**), which corresponds with the reduced friction coefficients (**Figure 4b**)
627 and equivalent friction force in the mixed regime for these samples (**Table 3**). However,
628 considering that these beads were not rolling, as discussed before, the beads appeared to
629 provide some degree of inhomogeneity perception, which might explain the relatively low
630 scores on the attribute 'smooth' ($p < 0.05$) as compared to that of their absence in the other
631 hydrogels, irrespective of particle size (**Figure 8**). It is worth noting that the sensory perception
632 of particles is not only dictated by the particle size, but also by its concentration, shape,
633 roughness and hardness of the particles as well as the properties of the matrix in which it is
634 dispersed. For example, the sensory threshold for particle size in chocolate is ~ 30 μm

(Afoakwa, Paterson, & Fowler, 2007) whereas for sharp-faceted silica particles it is as low as 2 μm (Engelen, et al., 2005) the be perceived as rough and/or gritty. Also, a thicker matrix can mask the sensory detection of particles (Imai, Hatae, & Shimada, 1995; Sala & Scholten, 2015). Thus, the observed low ratings in sensory smoothness might have resulted from these soft big CaA beads (≥ 300 μm) with sizes much above the sensory detection threshold, the inability of the *κ*C matrix to mask such perceptions as well as the absence of any ball-bearing effects.

It is worth highlighting that although the *κ*C hydrogels scored high on the sensory attribute 'smooth' (**Figure 8**), the friction coefficients of *κ*C hydrogel bolus filtrates were highest in the boundary regime ($\mu \sim 0.5$) (**Figure 4b**). Noteworthy is that the PDMS substrates used in this study for tribology were highly hydrophobic (even after pre-adsorption of artificial saliva), which might not have allowed efficient polymer-adsorption of the hydrophilic *κ*C hydrogel bolus particles remaining in the filtrate to the substrates and thus did not reduce friction significantly ($p > 0.05$). This might not be the case during real oral processing as the oral mucosa is highly hydrophilic because of the salivary coating (Laguna & Sarkar, 2017). Hence, one might consider introducing some degree of hydrophilicity in these soft PDMS substrates for doing oral tribology measurements in order to accurately understand this sensory smoothness scores for *κ*C hydrogels (Sarkar, et al., 2017a). Interestingly, the friction coefficients of the *κ*C hydrogel bolus fragments (particularly 3*κ*C) was considerably low ($\mu \sim 0.15$) in the boundary regime (**Figure 4a**, **Table 3**). This suggests that the 3*κ*C gel bolus fragments were responsible for acting as a solvated layer of lubricant to reduce viscous friction, as discussed previously, and consequently were rated high on the sensory attribute, 'smooth' (**Figure 8**).

For the attributes 'slippery' and 'salivating', the trend was not very clear for samples containing NaA or CaA (**Figure 8**), which might be associated with the rather difficult definitions and the unfamiliarity of the panel with these lubrication-related texture attributes.

660 This can also be seen in the Tucker-1 plots, see **Supplementary Figure 2**, where the attributes
661 'slippery' and salivating' showed rather random clustering patterns indicative of poor panel
662 agreement. It appears that insufficient training was provided to the participants on these
663 constructs for them to grasp the complexity of these attributes in novel semi-solid systems i.e.
664 the hydrogels with different textural complexity. Only samples containing NaA scored
665 significantly lower on 'salivating' as compared to that of *κ*C or *κ*C/LBG hydrogels ($p < 0.05$).
666 'Salivating' was defined as 'amount of saliva released during chewing' (**Table 2**). Therefore,
667 it is likely that panellists rated *κ*C or *κ*C/LBG hydrogels as more 'salivating' compared to that
668 of NaA samples ($p < 0.05$) as possibly a larger quantity of saliva was generated for cleansing
669 the residues of the stiffer hydrogel fragments (**Figure 1**). Similarly, samples containing NaA
670 and CaA (except 1.6*κ*C0.2CaA$_{300}$) scored significantly lower on the attribute 'slippery'
671 compared to that of *κ*C hydrogels ($p < 0.05$). This suggests that samples containing alginate
672 as biopolymer or beads did not slip easily and provided some sort of oral coating properties
673 due to the alginate itself or created a 'weeping' layer of water as a lubricant during tribological
674 shearing (Gong & Osada, 2002), as discussed in the previous section. The oral coating property
675 of alginates is in agreement with literature suggesting that alginate can create hydrogen bonds
676 with human salivary mucins through carboxyl–hydroxyl interactions (Cook, Bull, Methven,
677 Parker, & Khutoryanskiy, 2017; Shtenberg, et al., 2018).

678 In general, it can be concluded that all chewing-related attributes were largely
679 controlled by the fracture properties of the hydrogels, whereas the lubrication-related attributes
680 showed significant variations between the hydrogel samples and some of the lubrication-related
681 attributes corroborated the oral tribology results of the gel bolus filtrates in the mixed
682 lubrication regime. Noteworthy is that the relationship between fracture properties, tribology
683 and sensory analysis has been investigated in literature, particularly in emulsion gels
684 (Devezeaux de Lavergne, van Delft, van de Velde, van Boekel, & Stieger, 2015b; Liu, Stieger,

van der Linden, & van de Velde, 2016). Nevertheless, to our knowledge, this is the first study that has been carried out using descriptive sensory analysis focussing on textural attributes related to both chewing and lubrication in aqueous systems i.e. hydrogels with varying degree of textural complexity.

3.3. Relationship between the and sensory properties of the hydrogels

To understand the complex sensory perceptions in these hydrogels with or without inhomogeneity, an integrative approach of identifying interrelationships between sensory textural attributes and instrumental parameters rather than dependence on a single instrumental test is necessary. **Table 6** highlights the statistically significant correlation coefficients between the broad spectrum of mechanical parameters, i.e. fracture properties, apparent viscosity, μ in boundary and mixed lubrication regime, and the texture attributes.

Positive correlations were obtained between the chewing-related sensory attributes, i.e., 'firm', 'elastic', 'chewy' and 'cohesive' and the instrumental measures of fracture stress, fracture strain, fracture energy and viscosity at 50 s^{-1} (**Table 6**). The correlations of the fracture parameters with the chewing-related attributes are in agreement with previous literature dealing with emulsion gels (Devezeaux de Lavergne, et al., 2015a) and agarose gels (Barrangou, Drake, Daubert, & Foegeding, 2006). This suggests that firm samples, such as, *κ*C and *κ*C/LBG will require more stress to deform, particularly in the early stages of oral processing.

Interestingly, the lubrication-related sensory attribute 'salivating' also showed strong positive correlations with instrumental measures of fracture stress, fracture strain, fracture energy and viscosity at 50 s^{-1}, respectively. As discussed previously, the firm samples might have created residues/particles, which required increased salivary flow for oral cleansing (**Table 2**). Hence, it appears that the trained panel might have associated sensory 'salivating' with the quantity rather than the quality of saliva production. In addition, strong inverse

relationships were obtained between ‘pasty’, and ‘melting’ and the instrumental measures of fracture stress, fracture strain, fracture energy of the hydrogels and viscosity of boli at 50 s^{-1} ($p < 0.01$). In other words, ‘firm’ samples, such as κC or κC/LBG hydrogels might have created bolus fragments during the oral processing that were relatively stiff, retained their integrity and were not melting easily over the duration of the oral residence time. In addition, due to such fragment creation, firm samples were not perceived to be ‘pasty’ ($p < 0.01$) i.e. did not form a semi-solid continuous layer. Although the sensory attribute ‘smooth’ showed no correlations with either the fracture properties of the hydrogels or the viscosity of the boli, the sensory attribute ‘slippery’ showed a positive correlation with initial fracture stress and fracture strain, which suggests that the term ‘slippery’ had some association with early stages of oral processing, which was not expected ($p > 0.05$). Overall, clear relationships existed between all fracture properties of the hydrogels and rheology of the bolus fragments with lubrication-related attributes, such as ‘pasty’, ‘melting’ and ‘salivating’ that were perceived by the panellists during oral processing.

We now shift our focus to investigate whether µ of the hydrogel fragments and/or filtrates could predict the sensory dimensions of both chewing- and lubrication-related texture attributes (**Table 6**). As one might expect, no correlations existed between the chewing-related attributes and µ of bolus fragments/filtrates irrespective of the lubrication regimes. However, looking at the lubrication-related sensory attributes (**Table 6**), ‘pasty’ was inversely correlated with the µ of hydrogel bolus filtrates in the mixed lubrication regimes ($p < 0.05$). This further suggests that ‘pasty’ was most likely associated with the mouth-coating aspects during oral processing, as discussed previously. For example, samples with lower µ values (e.g. 1.5κC0.5NaA) in the boundary regime will be more lubricating and will thus be perceived as more ‘pasty’ forming an oral coating and/or ‘weeping’ layer of water, separating the oral surfaces from the asperity contacts. Although the signs of correlations in case of the tribology

735 experiments performed with hydrogel bolus fragments were similar to that of the hydrogel
736 bolus filtrate, no significance was observed in the former irrespective of the lubrication-related
737 attribute. This confirms that the bolus filtrates being thin-film had more relevance in the oral
738 tribology domain in this study when relating to the in-mouth sensory perception as compared
739 to that of the bolus gel fragments.

740 Interestingly, there was a tendency towards an inverse relationship of sensory 'melting'
741 to the μ of the hydrogel bolus filtrates in the mixed lubrication regime, however there was no
742 statistical significance (**Table 6**). Moreover, 'salivating' was positively correlated with the μ
743 of the bolus fragments ($p < 0.05$). This is in agreement with the explanation for the initial
744 fracture properties, which suggests that hydrogels scoring higher on 'salivating' were the
745 samples that generated more volume of saliva (**Table 2**). As can be expected, the generated
746 saliva was perhaps depleting the gel fragments or residues from the oral surfaces. Such
747 'depletion' of bolus fragments or residues from the oral surfaces might have resulted in
748 apparent surface asperity contacts, which may justify the positive correlation of 'salivating'
749 with friction coefficients as observed in **Table 6**. No relationships could be observed between
750 'smooth' and μ of bolus filtrates, which might be attributed to the inhomogeneity of samples,
751 such as the ones containing CaA beads. For the sensory attribute 'slippery', there was a positive
752 correlation with μ of hydrogel bolus filtrates in the mixed lubrication regime ($p < 0.05$) (**Table**
753 **6**).

754 It is worth highlighting this observed anomaly when relating the sensory attribute of
755 'slippery' to the tribology results. Previously, an inverse relationship of friction coefficient and
756 slipperiness in foods, i.e. $slipperiness\ \alpha\ \frac{1}{Viscous\ force + W\mu}$ (where W is the applied load in
757 tribology), has been postulated by Kokini (1987). However, this previous study by Kokini
758 (1987) was done with fat-rich low viscosity fluids, where 'slipperiness' could be perceived
759 easily due to 'fatty' or 'creamy mouthfeel'. In comparison, the current study has employed

semi-solid aqueous hydrogels and their corresponding bolus fragments and filtrates. Furthermore, 'slippery' perception was defined by the ease of sliding of the sample (**Table 2**). This suggests that highly slippery samples, such as 2κC gels (**Figure 8**) were sliding past the oral mucosa easily, which apparently resulted in having no fragments/ filtrate in the confinement, corroborating with the high μ values (**Figure 4b, Table 3**). Nevertheless, it is worth to emphasize that both 'slippery' and 'salivating' were difficult sensory terms for the panellists (**Figure 8**), as discussed before, and thus these correlations might be taken with some degree of precaution.

4. Conclusions

This study presents hydrogels as model semi-solid foods, where systematic manipulation of the structural properties was used to investigate the relationship between mechanical (instrumentally measured) and sensory aspects of oral processing. A range of hydrogels with varying degrees of structural complexity was evaluated using uniaxial compression test of the hydrogels, flow curves and tribology of gel boli (after simulated oral processing) as well the sensory properties, which was investigated using descriptive sensory analysis. Tribology of the bolus fragments and filtrates were explained using theoretical "repulsion-adsorption" model highlighting the role of opposing surfaces (PDMS, gels). A clear correlation was obtained between the initial fracture properties of the hydrogels, viscosity of the bolus fragments and all chewing-related texture attributes i.e. 'firm', 'elastic', 'chewy' and 'cohesive'. Interestingly, all fracture attributes and boli viscosity showed positive correlation to the relatively novel lubrication-related texture attributes, such as 'salivating' and inverse correlations with both 'pasty' and 'melting'. The coefficient of friction of the bolus filtrates in the mixed lubrication regime showed inverse correlations with the lubrication-related attributes, such as sensory 'pasty' and positive correlations with 'slippery' and 'salivating'.

However, our experimental design could not establish a significant inverse correlation between sensory 'smooth' and the friction coefficients, which is largely attributed to the inhomogeneity of the samples employed in the study. Novel findings from this study suggests that lubrication-related attributes were perceived during both early and later stages of oral processing and thus relationships existed with initial fracture properties of gels, boli viscosity and boli tribology and not only to boli tribology, as hypothesized initially. Future studies should focus on further training of panel members particularly with respect to lubrication-related texture attributes. In addition, more independent systematic studies with hydrogels with varying degrees of structural complexity at micro- to macro-scale are needed to clearly establish the tribology-sensory relationships particularly at the later stages of oral processing.

Acknowledgements

We thank Siti Ahmad for her help in formulating the preliminary hydrogels, as well as we thank all participants for their time and willingness to taste the model hydrogels. Author (EK) acknowledges University of Leeds 110 Anniversary Research Scholarship with matched support from Mars Wrigley Confectionery for funding her PhD studies.

References

Afoakwa, E. O., Paterson, A., & Fowler, M. (2007). Factors influencing rheological and textural qualities in chocolate – a review. Trends in Food Science & Technology, 18(6), 290-298.

Barrangou, L. M., Drake, M., Daubert, C. R., & Foegeding, E. A. (2006). Textural properties of agarose gels. II. Relationships between rheological properties and sensory texture. Food Hydrocolloids, 20(2), 196-203.

809 Bongaerts, J. H. H., Cooper-White, J. J., & Stokes, J. R. (2009). Low biofouling chitosan-
810 hyaluronic acid multilayers with ultra-low friction coefficients. Biomacromolecules,
811 10(5), 1287-1294.

812 Bongaerts, J. H. H., Fourtouni, K., & Stokes, J. R. (2007a). Soft-tribology: Lubrication in a
813 compliant PDMS–PDMS contact. Tribology International, 40(10–12), 1531-1542.

814 Bongaerts, J. H. H., Rossetti, D., & Stokes, J. R. (2007b). The lubricating properties of human
815 whole saliva. Tribology letters, 27(3), 277-287.

816 Chen, J., & Stokes, J. R. (2012). Rheology and tribology: Two distinctive regimes of food
817 texture sensation. Trends in Food Science & Technology, 25(1), 4-12.

818 Cook, S. L., Bull, S. P., Methven, L., Parker, J. K., & Khutoryanskiy, V. V. (2017).
819 Mucoadhesion: A food perspective. Food Hydrocolloids, 72, 281-296.

820 Czaczyk, K., Olejnik, A., & Trojanowska, K. (1999). The influence of LBG addition to
821 carrageenan on the mechanical stability of the gel and the fermentative activity of
822 immobilized propionic acid bacteria. Acta Biotechnologica, 19(2), 147-156.

823 de Vicente, J., Stokes, J. R., & Spikes, H. A. (2005). The Frictional Properties of Newtonian
824 Fluids in Rolling–Sliding soft-EHL Contact. Tribology Letters, 20(3), 273-286.

825 Dea, I. C. M., & Morrison, A. (1975). Chemistry and Interactions of Seed Galactomannans. In
826 R. S. Tipson & D. Horton (Eds.), Advances in Carbohydrate Chemistry and
827 Biochemistry (Vol. 31, pp. 241-312): Academic Press.

828 Devezeaux de Lavergne, M., Strijbosch, V. M. G., Van den Broek, A. W. M., Van de Velde,
829 F., & Stieger, M. (2016). Uncoupling the Impact of Fracture Properties and
830 Composition on Sensory Perception of Emulsion-Filled Gels. Journal of Texture
831 Studies, 47(2), 92-111.

832 Devezeaux de Lavergne, M., van de Velde, F., van Boekel, M. A. J. S., & Stieger, M. (2015a).
833 Dynamic texture perception and oral processing of semi-solid food gels: Part 2: Impact
834 of breakdown behaviour on bolus properties and dynamic texture perception. Food
835 Hydrocolloids, 49, 61-72.

836 Devezeaux de Lavergne, M., van Delft, M., van de Velde, F., van Boekel, M. A. J. S., & Stieger,
837 M. (2015b). Dynamic texture perception and oral processing of semi-solid food gels:
838 Part 1: Comparison between QDA, progressive profiling and TDS. Food
839 Hydrocolloids, 43, 207-217.

840 Dunstan, D. E., Chen, Y., Liao, M. L., Salvatore, R., Boger, D. V., & Prica, M. (2001).
841 Structure and rheology of the κ-carrageenan/locust bean gum gels. Food Hydrocolloids,
842 15(4-6), 475-484.

843 Engelen, L., de Wijk, R. A., van der Bilt, A., Prinz, J. F., Janssen, A. M., & Bosman, F. (2005).
844 Relating particles and texture perception. Physiology & Behavior, 86(1), 111-117.

845 Field, A. (2017). Discovering statistics using IBM SPSS statistics London, United Kingdom:
846 Sage Publications Ltd.

847 Foegeding, E. A., Daubert, C. R., Drake, M. A., Essick, G., Trulsson, M., Vinyard, C. J., &
848 Van De Velde, F. (2011). A comprehensive approach to understanding textural
849 properties of semi- and soft-solid foods. Journal of Texture Studies, 42(2), 103-129.

850 Funami, T., Ishihara, S., Nakauma, M., Kohyama, K., & Nishinari, K. (2012). Texture design
851 for products using food hydrocolloids. Food Hydrocolloids, 26(2), 412-420.

852 Garrec, D. A., & Norton, I. T. (2013). Kappa carrageenan fluid gel material properties. Part 2:
853 Tribology. Food Hydrocolloids, 33(1), 160-167.

854 Goh, K. K. T., Sarkar, A., & Singh, H. (2008). Chapter 12 - Milk protein–polysaccharide
855 interactions. In Milk Proteins (pp. 347-376). San Diego: Academic Press.

856 Goh, K. K. T., Sarkar, A., & Singh, H. (2014). Chapter 13 - Milk Protein–Polysaccharide
857 Interactions. In Milk Proteins (Second edition) (pp. 387-419). San Diego: Academic
858 Press.

859 Gong, J., & Osada, Y. (1998). Gel friction: A model based on surface repulsion and adsorption.
860 The Journal of Chemical Physics, 109(18), 8062-8068.

861 Gong, J. P. (2006). Friction and lubrication of hydrogels-its richness and complexity. Soft
862 Matter, 2(7), 544-552.

863 Gong, J. P., Kagata, G., Iwasaki, Y., & Osada, Y. (2001). Surface friction of polymer gels: 1.
864 Effect of interfacial interaction. Wear, 251(1), 1183-1187.

865 Gong, J. P., Kagata, G., & Osada, Y. (1999). Friction of gels. 4. Friction on charged gels. The
866 Journal of Physical Chemistry B, 103(29), 6007-6014.

867 Gong, J. P., & Osada, Y. (2002). Surface friction of polymer gels. Progress in Polymer Science,
868 27(1), 3-38.

869 Hayakawa, F., Kazami, Y., Ishihara, S., Nakao, S., Nakauma, M., Funami, T., Nishinari, K., &
870 Kohyama, K. (2014). Characterization of eating difficulty by sensory evaluation of
871 hydrocolloid gels. Food Hydrocolloids, 38, 95-103.

872 Hori, K., Hayashi, H., Yokoyama, S., Ono, T., Ishihara, S., Magara, J., Taniguchi, H., Funami,
873 T., Maeda, Y., & Inoue, M. (2015). Comparison of mechanical analyses and tongue
874 pressure analyses during squeezing and swallowing of gels. Food Hydrocolloids, 44,
875 145-155.

876 Hutchings, J. B., & Lillford, P. J. (1988). The perception of food texture - the philosophy of
877 the breakdown path. Journal of Texture Studies, 19(2), 103-115.

878 Imai, E., Hatae, K., & Shimada, A. (1995). Oral perception of grittiness: Effect of particle size
879 and concentration of the dispersed particles and the dispersion medium. Journal of
880 Texture Studies, 26(5), 561-576.

881 Ishihara, S., Nakauma, M., Funami, T., Odake, S., & Nishinari, K. (2011). Viscoelastic and
882 fragmentation characters of model bolus from polysaccharide gels after instrumental
883 mastication. Food Hydrocolloids, 25(5), 1210-1218.

884 Johnson, K. L. (2009). Normal Contact Of Elastic Solids: Hertz Theory. In Contact Mechanics:
885 Cambridge University Press.

886 Johnston, I. D., McCluskey, D. K., Tan, C. K. L., & Tracey, M. C. (2014). Mechanical
887 characterization of bulk Sylgard 184 for microfluidics and microengineering. Journal
888 of Micromechanics and Microengineering, 24(3).

889 Kohyama, K., Hayakawa, F., Kazami, Y., Ishihara, S., Nakao, S., Funami, T., & Nishinari, K.
890 (2015). Electromyographic texture characterization of hydrocolloid gels as model foods
891 with varying mastication and swallowing difficulties. Food Hydrocolloids, 43, 146-
892 152.

893 Kokini, J. L. (1987). The physical basis of liquid food texture and texture-taste interactions.
894 Journal of Food Engineering, 6(1), 51-81.

895 Krop, E. M., Hetherington, M. M., Nekitsing, C., Miquel, S., Postelnicu, L., & Sarkar, A.
896 (2018). Influence of oral processing on appetite and food intake – A systematic review
897 and meta-analysis. Appetite, 125, 253-269.

898 Laguna, L., Farrell, G., Bryant, M., Morina, A., & Sarkar, A. (2017a). Relating rheology and
899 tribology of commercial dairy colloids to sensory perception. Food & Function, 8(2),
900 563-573.

Laguna, L., Hetherington, M. M., Chen, J., Artigas, G., & Sarkar, A. (2016). Measuring eating capability, liking and difficulty perception of older adults: A textural consideration. Food Quality and Preference, 53, 47-56.

Laguna, L., & Sarkar, A. (2016). Influence of mixed gel structuring with different degrees of matrix inhomogeneity on oral residence time. Food Hydrocolloids, 61, 286-299.

Laguna, L., & Sarkar, A. (2017). Oral tribology: update on the relevance to study astringency in wines. Tribology - Materials, Surfaces & Interfaces, 11(2), 116-123.

Laguna, L., Sarkar, A., Bryant, M. G., Beadling, A. R., Bartolomé, B., & Victoria Moreno-Arribas, M. (2017b). Exploring mouthfeel in model wines: Sensory-to-instrumental approaches. Food Research International, 102, 478-486.

Larsen, B. E., Bjørnstad, J., Pettersen, E. O., Tønnesen, H. H., & Melvik, J. E. (2015). Rheological characterization of an injectable alginate gel system. BMC Biotechnology, 15, 29.

Liu, K., Stieger, M., van der Linden, E., & van de Velde, F. (2016). Effect of microparticulated whey protein on sensory properties of liquid and semi-solid model foods. Food Hydrocolloids, 60, 186-198.

Liu, K., Tian, Y., Stieger, M., van der Linden, E., & van de Velde, F. (2016). Evidence for ball-bearing mechanism of microparticulated whey protein as fat replacer in liquid and semi-solid multi-component model foods. Food Hydrocolloids, 52, 403-414.

Madsen, J. B., Sotres, J., Pakkanen, K. I., Efler, P., Svensson, B., Abou Hachem, M., Arnebrant, T., & Lee, S. (2016). Structural and mechanical properties of thin films of bovine submaxillary mucin versus porcine gastric mucin on a hydrophobic surface in aqueous solutions. Langmuir, 32(38), 9687-9696.

924 Minekus, M., Alminger, M., Alvito, P., Ballance, S., Bohn, T., Bourlieu, C., Carriere, F.,
925 Boutrou, R., Corredig, M., Dupont, D., Dufour, C., Egger, L., Golding, M., Karakaya,
926 S., Kirkhus, B., Le Feunteun, S., Lesmes, U., Macierzanka, A., Mackie, A., Marze, S.,
927 McClements, D. J., Menard, O., Recio, I., Santos, C. N., Singh, R. P., Vegarud, G. E.,
928 Wickham, M. S. J., Weitschies, W., & Brodkorb, A. (2014). A standardised static in
929 vitro digestion method suitable for food - an international consensus. Food & Function,
930 5(6), 1113-1124.

931 Miquel-Kergoat, S., Azais-Braesco, V., Burton-Freeman, B., & Hetherington, M. M. (2015).
932 Effects of chewing on appetite, food intake and gut hormones: A systematic review and
933 meta-analysis. Physiology & Behavior, 151, 88-96.

934 Morell, P., Chen, J., & Fiszman, S. (2017). The role of starch and saliva in tribology studies
935 and the sensory perception of protein-added yogurts. Food & Function, 8(2), 545-553.

936 Peleg, M. (1984). A note on the various strain measures at large compressive deformations.
937 Journal of Texture Studies, 15(4), 317-326.

938 Pradal, C., & Stokes, J. R. (2016). Oral tribology: bridging the gap between physical
939 measurements and sensory experience. Current Opinion in Food Science, 9, 34-41.

940 Prakash, S., Tan, D. D. Y., & Chen, J. (2013). Applications of tribology in studying food oral
941 processing and texture perception. Food Research International, 54(2), 1627-1635.

942 Puttock, M. J., & Thwaite, E. G. (1969). Elastic Compression of Spheres and Cylinders at Point
943 and Line Contact. National Standards Laboratory Technical Paper, 25.

944 Sala, G., & Scholten, E. (2015). Chapter 5 - Instrumental characterisation of textural properties
945 of fluid food A2 - Chen, Jianshe. In A. Rosenthal (Ed.), Modifying Food Texture (pp.
946 107-131): Woodhead Publishing.

947 Santagiuliana, M., Piqueras-Fiszman, B., van der Linden, E., Stieger, M., & Scholten, E.
948 (2018). Mechanical properties affect detectability of perceived texture contrast in
949 heterogeneous food gels. Food Hydrocolloids, 80, 254-263.

950 Sarkar, A., Goh, K. K. T., & Singh, H. (2009). Colloidal stability and interactions of milk-
951 protein-stabilized emulsions in an artificial saliva. Food Hydrocolloids, 23(5), 1270-
952 1278.

953 Sarkar, A., Kanti, F., Gulotta, A., Murray, B. S., & Zhang, S. (2017a). Aqueous lubrication,
954 structure and rheological properties of whey protein microgel particles. Langmuir,
955 33(51), 14699-14708.

956 Sarkar, A., & Singh, H. (2012). Oral behaviour of food emulsions. In Food Oral Processing
957 (pp. 111-137): Wiley-Blackwell.

958 Sarkar, A., Ye, A., & Singh, H. (2017b). Oral processing of emulsion systems from a colloidal
959 perspective. Food & Function, 8(2), 511-521.

960 Schipper, R. G., Silletti, E., & Vingerhoeds, M. H. (2007). Saliva as research material:
961 biochemical, physicochemical and practical aspects. Arch Oral Biol, 52(12), 1114-
962 1135.

963 Shtenberg, Y., Goldfeder, M., Prinz, H., Shainsky, J., Ghantous, Y., Abu El-Naaj, I., Schroeder,
964 A., & Bianco-Peled, H. (2018). Mucoadhesive alginate pastes with embedded
965 liposomes for local oral drug delivery. International Journal of Biological
966 Macromolecules, 111, 62-69.

967 Stading, M., & Hermansson, A.-M. (1993). Rheological behaviour of mixed gels of κ-
968 carrageenan-locust bean gum. Carbohydrate Polymers, 22(1), 49-56.

969 Steele, C. M., & Van Lieshout, P. (2009). Tongue movements during water swallowing in
970 healthy young and older adults. J Speech Lang Hear Res, 52(5), 1255-1267.

971 Stokes, J. R., Boehm, M. W., & Baier, S. K. (2013). Oral processing, texture and mouthfeel:
972 From rheology to tribology and beyond. Current Opinion in Colloid & Interface
973 Science, 18(4), 349-359.

974 Stokes, J. R., Macakova, L., Chojnicka-Paszun, A., de Kruif, C. G., & de Jongh, H. H. J. (2011).
975 Lubrication, adsorption, and rheology of aqueous polysaccharide solutions. Langmuir,
976 27(7), 3474-3484.

977 Tang, J., Larsen, D. S., Ferguson, L. R., & James, B. J. (2016). The effect of textural complexity
978 of solid foods on satiation. Physiology & Behavior, 163, 17-24.

979 Tomic, O., Luciano, G., Nilsen, A., Hyldig, G., Lorensen, K., & Næs, T. (2010). Analysing
980 sensory panel performance in a proficiency test using the PanelCheck software.
981 European Food Research and Technology, 230, 497-511.

982 van Stee, M.-A., de Hoog, E., & van de Velde, F. (2017). Oral Parameters Affecting Ex-vivo
983 Tribology. Biotribology, 11, 84-91.

984 Vijay, A., Inui, T., Dodds, M., Proctor, G., & Carpenter, G. (2015). Factors that influence the
985 extensional rheological property of saliva. PLOS ONE, 10(8), e0135792.

986 Yakubov, G. E., McColl, J., Bongaerts, J. H. H., & Ramsden, J. J. (2009). Viscous boundary
987 lubrication of hydrophobic surfaces by mucin. Langmuir, 25(4), 2313-2321.
988

Figure 1.

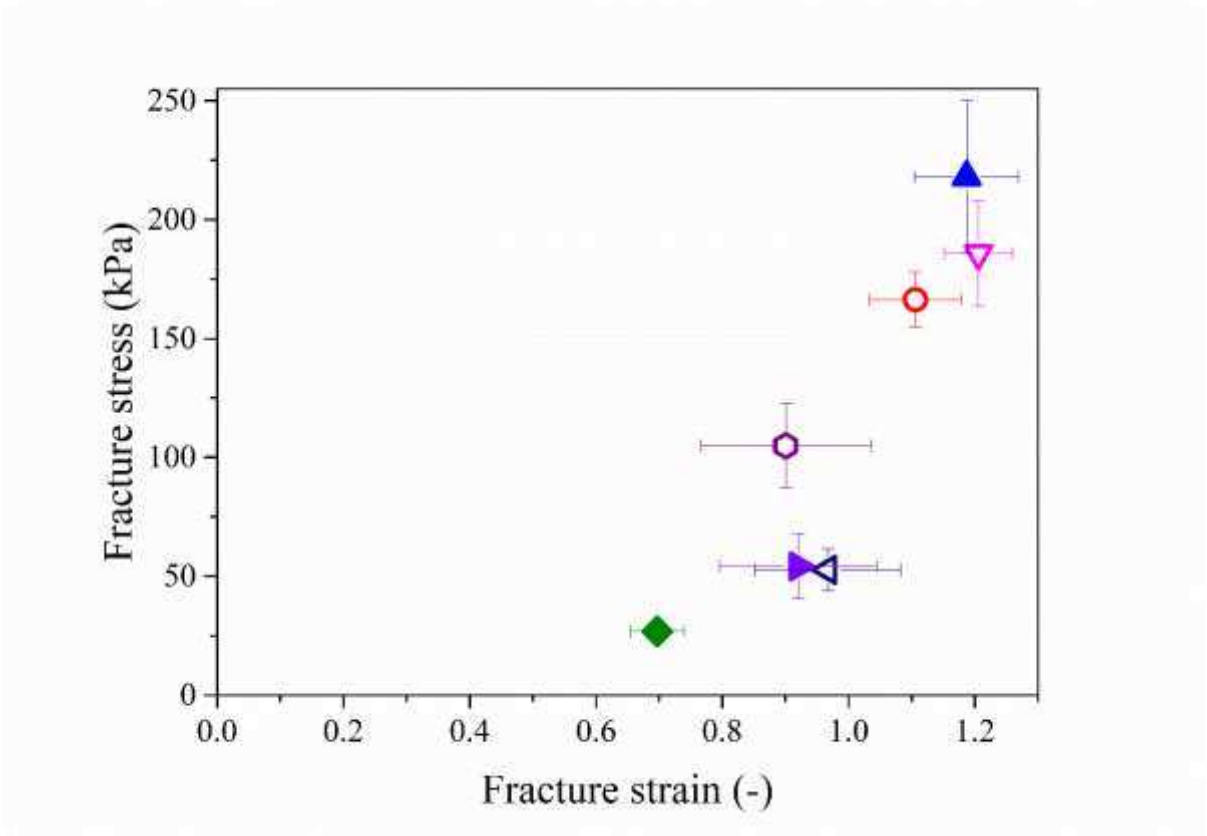
Fracture stress (kPa)
250
200
150
100
50
0
0.0
0.2
0.4
0.6
0.8
1.0
1.2
Fracture strain (-)

Figure 2.

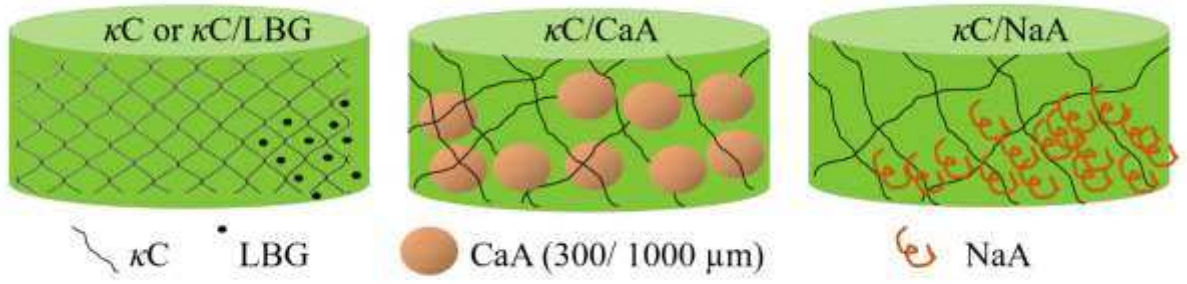

Figure 3.

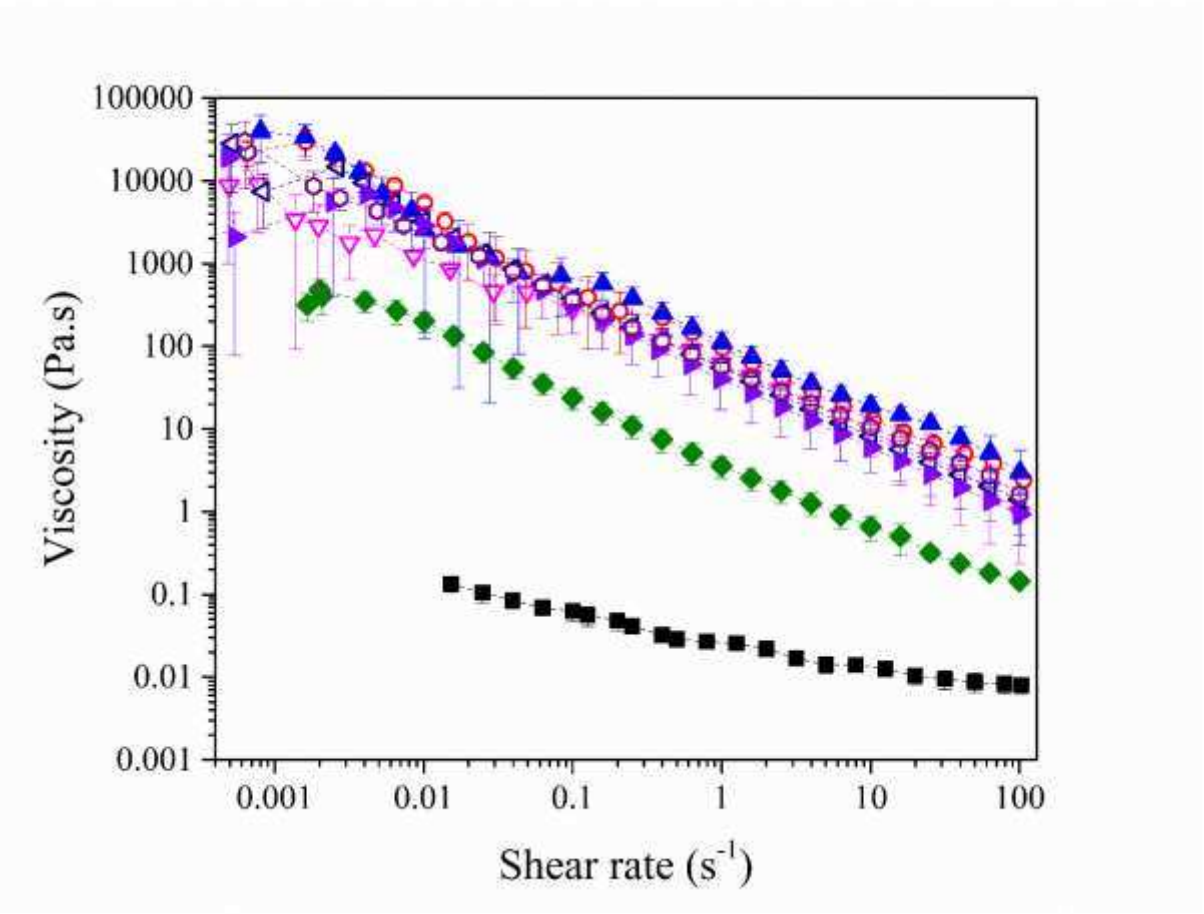
Viscosity (Pa.s)
100000
10000
1000
100
10
1
0.1
0.01
0.001
0.001
0.01
0.1
1
10
100
Shear rate (s-1)

Figure 4.

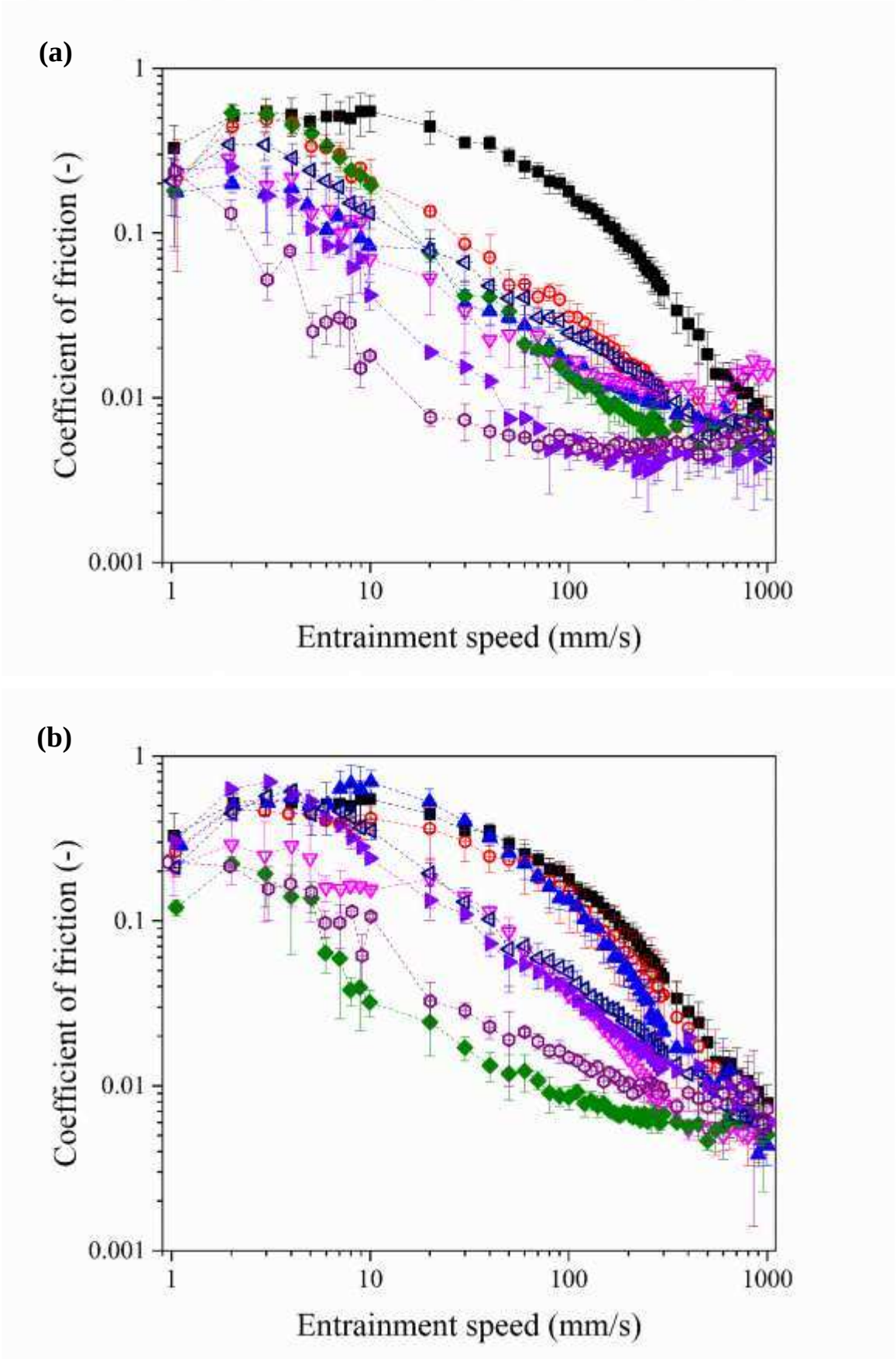
(a)
Coefficient of friction (-)
1
0.1
0.01
0.001
1
10
100
1000
Entrainment speed (mm/s)
(b)
Coefficient of friction (-)
1
0.1
0.01
0.001
1
10
100
1000
Entrainment speed (mm/s)

Figure 5.

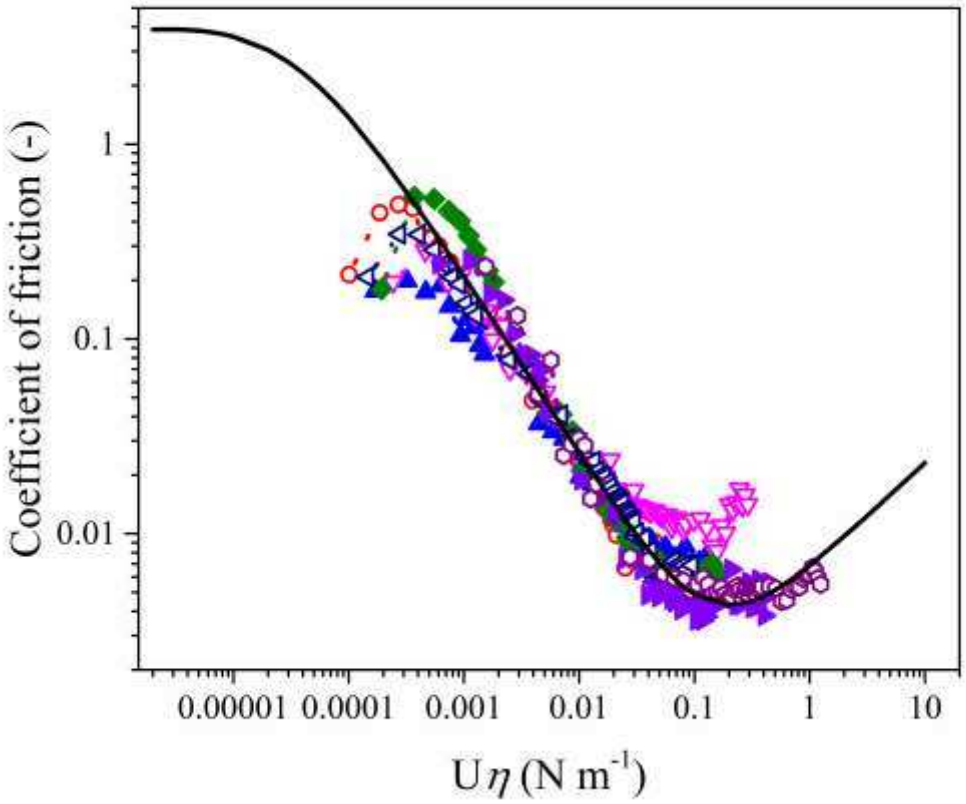
Coefficient of friction (-)
1
0.1
0.01
0.00001
0.0001
0.001
0.01
0.1
1
10
Uη (N m-1)

Figure 6.

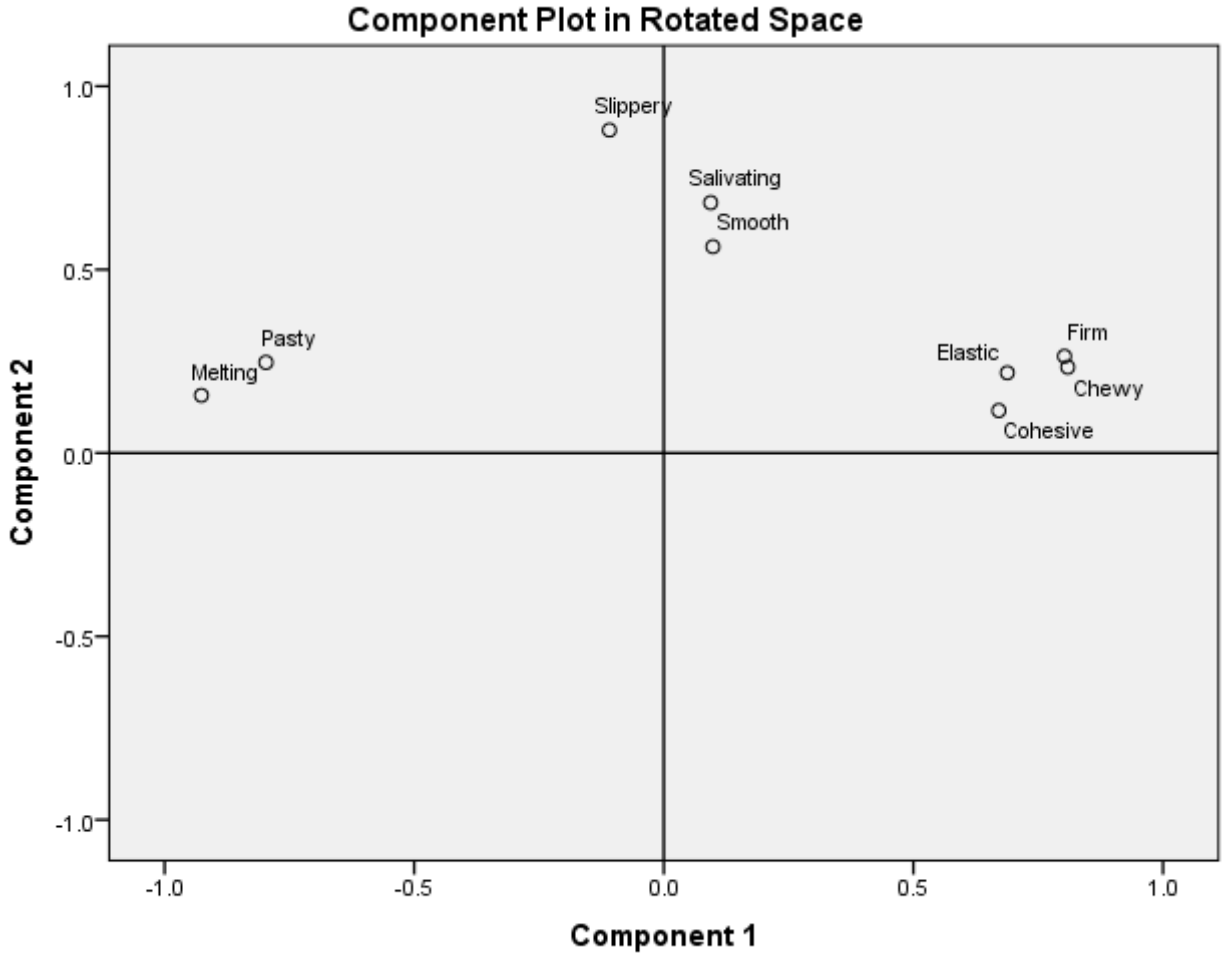
Component Plot in Rotated Space
Slippery
Salivating
Smooth
Pasty
Melting
Elastic
Firm
Chewy
Cohesive
1.0
0.5
0.0
-0.5
-1.0
Component 2
-1.0
-0.5
0.0
0.5
1.0
Component 1

Figure 7.

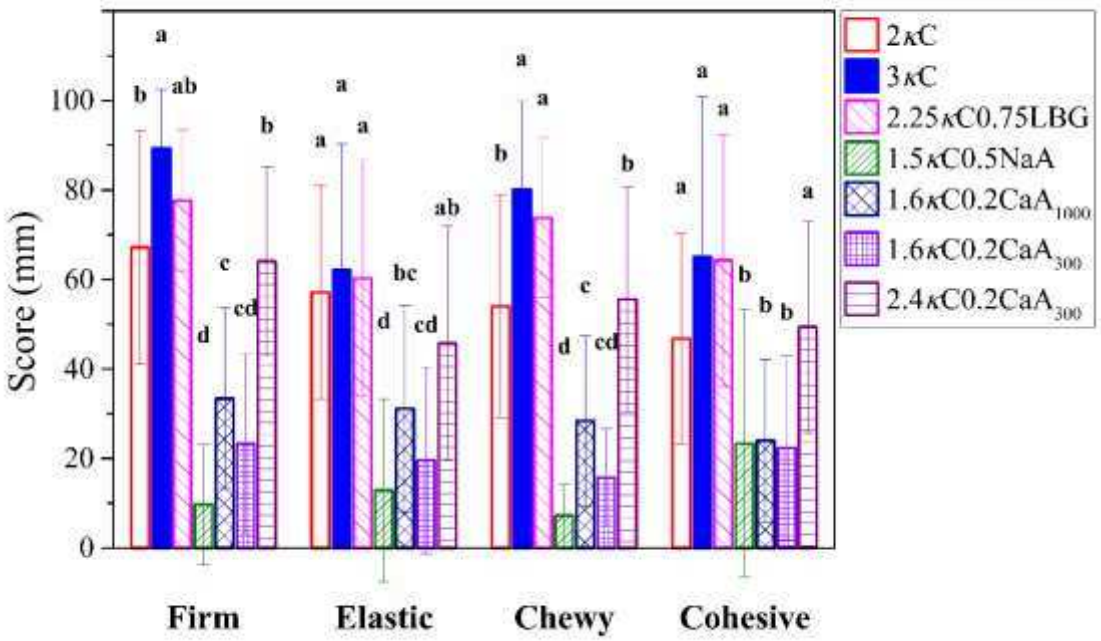
Score (mm)
0
20
40
60
80
100
Firm
Elastic
Chewy
Cohesive
2κC
3κC
2.25κC0.75LBG
1.5κC0.5NaA
1.6κC0.2CaA1000
1.6κC0.2CaA300
2.4κC0.2CaA300

Figure 8.

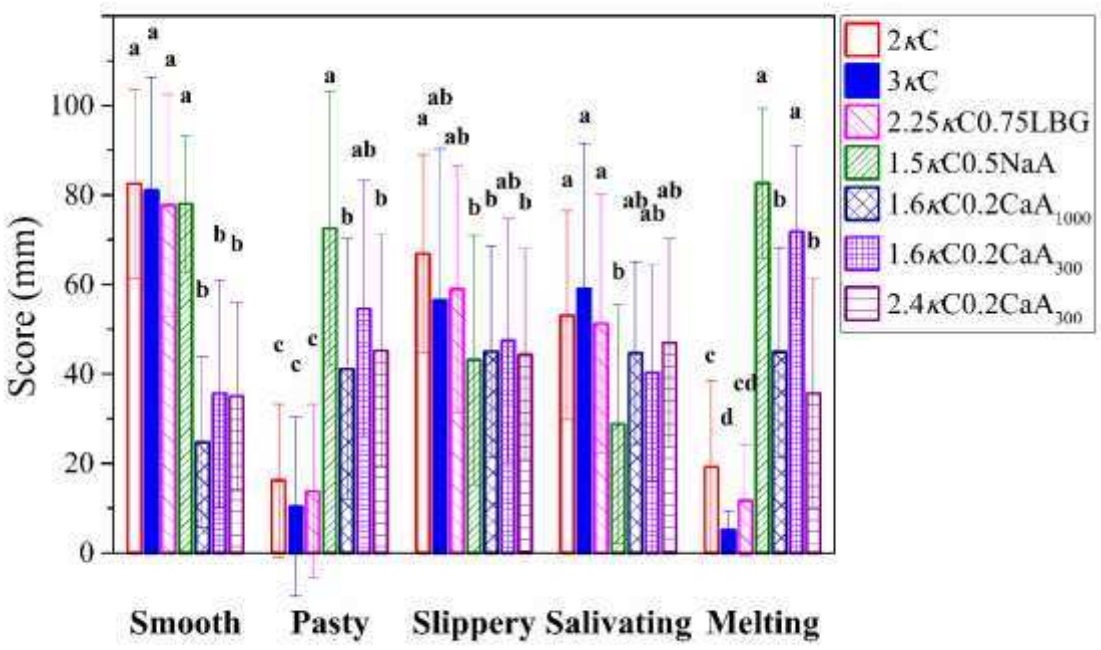
Score (mm)
0
20
40
60
80
100
Smooth
Pasty
Slippery
Salivating
Melting
2κC
3κC
2.25κC0.75LBG
1.5κC0.5NaA
1.6κC0.2CaA1000
1.6κC0.2CaA300
2.4κC0.2CaA300

Captions for Figures

Figure 1. Fracture stress and strain of 2κC (○), 3κC (▲), 2.25κC0.75LBG (▽), 1.5κC0.5NaA (◆), 1.6κC0.2CaA$_{1000}$ (◁), 1.6κC0.2CaA$_{300}$ (▶) and 2.4κC0.2CaA$_{300}$ (⬡) hydrogels in uniaxial compression test. Data points represent the average of at least three measurements on four different preparation days. Error bars indicate the standard deviation.

Figure 2. Schematic representation of the hydrogels.

Figure 3. Flow curves of artificial saliva (■), 2κC (○), 3κC (▲), 2.25κC0.75LBG (▽), 1.5κC0.5NaA (◆), 1.6κC0.2CaA$_{1000}$ (◁), 1.6κC0.2CaA$_{300}$ (▶) and 2.4κC0.2CaA$_{300}$ (⬡) gel bolus fragments as a function of shear rate at 37 °C. Data points represent the average of at least three measurements. Error bars indicate the standard deviation.

Figure 4. Friction coefficients of 2κC (○), 3κC (▲), 2.25κC0.75LBG (▽), 1.5κC0.5NaA (◆), 1.6κC0.2CaA$_{1000}$ (◁), 1.6κC0.2CaA$_{300}$ (▶) and 2.4κC0.2CaA$_{300}$ (⬡) gel bolus fragments (a) and gel bolus filtrates (after filtering out the larger fragments) (b), respectively, after simulated oral processing in presence artificial saliva (■), at 37 °C as a function of entrainment speed. Data points represent the average of at least three measurements. Error bars indicate the standard deviation.

Figure 5. Stribeck master curve for 2κC (○), 3κC (▲), 2.25κC0.75LBG (▽), 1.5κC0.5NaA (◆), 1.6κC0.2CaA$_{1000}$ (◁), 1.6κC0.2CaA$_{300}$ (▶) and 2.4κC0.2CaA$_{300}$ (⬡) gel bolus fragments as

a function of the product of viscosity and entrainment speed component ($U\eta$). The black solid line is the best fit to the data using Eq (13)

Figure 6. Principal component analysis (PCA) of all texture attributes obtained in the descriptive sensory analysis. Principal component 1 (PC1) represents 48.5% and PC2 15.6% of the variance in the data.

Figure 7. The ratings of the chewing-related attributes obtained from QDA profiling of the gels. Data points represent the average of the gels evaluated in triplicate by 11 panelists. Error bars indicate the standard deviation and bars within one attribute with different lower case letters denote a statistically significant difference ($p < 0.05$).

Figure 8. The ratings of the lubrication-related attributes obtained from QDA profiling of the gels. Data points represent the average of the gels evaluated in triplicate by 11 panelists. Error bars indicate the standard deviation and bars within one attribute with different lower case letters denote a statistically significant difference ($p < 0.05$).

Table 1.

Hydrogel samples	κ-carrageenan (wt%)	Locust bean gum (wt%)	Na-alginate (wt%)	Ca-alginate beads (wt%)	Water (wt%)
2*κ*C	2				97
3*κ*C	3				96
2.25*κ*C0.75LBG	2.25	0.75			96
1.5*κ*C0.5NaA	1.5		0.5		97
1.6*κ*C0.2CaA$_{1000}$	1.6			0.2	97
1.6*κ*C0.2CaA$_{300}$	1.6			0.2	97
2.4*κ*C0.2CaA$_{300}$	2.4			0.2	96

* All hydrogels contained 0.5 wt% green food colouring and 0.5 wt% peppermint flavouring. The two *κ*-carrageenan hydrogels contained 0.145 wt% KCl. The composition of the mixed hydrogels containing Ca-alginate beads was determined based on the ratio *between κ*-carrageenan gel matrix (2 or 3 wt%) and Ca-alginate beads (1 wt%), irrespective of bead size.

Table 2.

Textural attributes from QDA profiling	Definition
Smooth	Degree of abrasiveness of the products surface as perceived by the tongue
Firm	The force needed to compress the sample between tongue and palate (hardness)
Elastic	The ease in which the sample bounces back after chewing (springiness)/force with which the sample returns to its original shape after partial compression (without fracture) between the tongue and palate
Chewy	The amount of chews needed to break down the sample to be ready for swallowing
Cohesiveness	Degree to which the samples deforms/holds together rather than crumbles/breaks/ruptures (it conforms to the palate rather than shears)
Pasty	The sensation of the presence of wet/soft (immiscible) solids in the mouth (muddy)
Slippery	The ease in which the sample slides through the mouth during chewing (slimy)
Salivating	The amount of saliva released during chewing
Melting	The amount of sample that dissolves/disappears over time (loss of structure in the mouth) rather than cracking or breaking apart

Table 3.

Samples	Friction force of the gel bolus fragments (N)				Friction force of the gel bolus filtrate (N)			
	Boundary lubrication regime (3 mm/s)		Mixed lubrication regime (50 mm/s)		Boundary lubrication regime (3 mm/s)		Mixed lubrication regime (50 mm/s)	
	Mean	SD	Mean	SD	Mean	SD	Mean	SD
Artificial saliva	1.097^{a}	0.211	0.585^{a}	0.071	1.097^{a}	0.211	0.585^{a}	0.071
2*κ*C	0.978^{ab}	0.179	0.096^{b}	0.024	0.928^{ab}	0.067	0.469^{a}	0.069
3*κ*C	0.348^{cd}	0.146	0.061^{b}	0.010	1.042^{a}	0.047	0.515^{a}	0.059
2.25*κ*C0.75LBG	0.387^{cd}	0.076	0.049^{b}	0.018	0.498^{bc}	0.301	0.172^{b}	0.036
1.5*κ*C0.5NaA	1.046^{ab}	0.125	0.067^{b}	0.011	0.386^{c}	0.143	0.024^{b}	0.007
1.6*κ*C0.2CaA$_{1000}$	0.687^{bc}	0.135	0.080^{b}	0.017	1.141^{a}	0.103	0.135^{b}	0.055
1.6*κ*C0.2CaA$_{300}$	0.338^{cd}	0.168	0.015^{b}	0.002	1.393^{a}	0.003	0.113^{b}	0.039
2.4*κ*C0.2CaA$_{300}$	0.104^{d}	0.026	0.012^{b}	0.003	0.313^{c}	0.112	0.038^{b}	0.018

Table 4.

Samples	**$N_{particle}$**	**$F_{particle}$ (N)**	**α (mm)**
1.6κC0.2CaA1000	0.5	3.90	18.3
1.6κC0.2CaA300	5.7	0.35	5.5
2.4κC0.2CaA300	5.7	0.35	5.5

Table 5.

	PC 1	PC 2
Smooth	.098	.562
Firm	.803	.264
Elastic	.688	.219
Chewy	.809	.234
Cohesive	.671	.116
Pasty	-.797	.247
Slippery	-.109	.880
Salivating	.094	.682
Melting	-.926	.157

Table 6.

		Smooth	Firm	Elastic	Chewy	Cohesive	Pasty	Slippery	Salivating	Melting	Fracture stress	Fracture strain	Fracture Energy	Viscosity at 50 s^{-1} shear rate	μ at 50 mm/s	μ at 3 mm/s	μ at 50 mm/s	μ at 3 mm/s
Sensory	**Smooth**																	
	Firm	0.40																
	Elastic	0.44	0.98															
	Chewy	0.41	0.99	0.98														
	Cohesive	0.53	0.96	0.94	0.98													
	Pasty	-0.43	-0.92	-0.95	-0.91	-0.84												
	Slippery	0.66	0.68	0.77	0.64	0.63	-0.84											
	Salivating	0.25	0.94	0.94	0.91	0.82	-0.95	0.71										
	Melting	-0.38	-0.97	-0.99	-0.97	-0.91	0.97	-0.73	-0.96									
Texture analysis	**Fracture stress**	0.59	0.96	0.96	0.95	0.95	-0.94	0.80	0.91	-0.94								
	Fracture strain	0.36	0.87	0.90	0.87	0.80	-0.98	0.80	0.92	-0.92	0.91							
	Fracture Energy	0.55	0.89	0.87	0.87	0.84	-0.88	0.72	0.90	-0.87	0.94	0.82						
Rheology	**Viscosity at 50 s^{-1} shear rate**	0.30	0.91	0.89	0.88	0.80	-0.90	0.67	0.98	-0.91	0.80	0.86	0.95					
Tribology, gel bolus filtrate	**μ at 50 mm/s**	0.56	0.68	0.71	0.63	0.57	-0.80	0.82	0.79	-0.72	0.79	0.74	0.90	0.85				
	μ at 3 mm/s	-0.30	-0.11	-0.11	-0.16	-0.30	-0.15	0.14	0.22	0.04	-0.03	0.25	0.14	0.24	0.39			
Tribology, gel bolus fragments	**μ at 50 mm/s**	0.47	0.06	0.19	0.05	0.00	-0.31	0.48	0.16	-0.24	0.18	0.22	0.25	0.16	0.56	0.15		
	μ at 3 mm/s	0.42	-0.44	-0.31	-0.45	-0.42	0.22	0.17	-0.40	0.31	-0.28	-0.30	-0.23	-0.37	0.18	0.34	0.81	

Captions for Tables

Table 1. Final composition of the hydrogels.

Table 2. List of attributes and descriptions as included in the QDA profiling.

Table 3. Friction force (N) for the gel bolus fluid (thin liquid) after filtering out the larger fragments at 3 mm/s (boundary lubrication regime) and 50 mm/s (mixed lubrication regime) entrainment speed and 37 °C. The samples were prepared using simulated oral processing in the presence of artificial saliva, and compared to artificial saliva as a control measure. A different lower case letter denotes a statistically significant difference ($p < 0.05$).

Table 4. Elastic compression of the CaA beads based on 10% particle entrainment.

Table 5. Pattern matrix from the Principal Component Analysis (PCA). The Oblimin with Kaiser Normalisation rotation method was applied and the rotation converged in 5 iterations. Highlighted in red shows the sensory attributes best represented in PC1 and PC2 (> 0.500).

Table 6. Pearson's correlations of sensory attributes (QDA) and physical properties (large deformation rheology, apparent viscosity and coefficient of friction) of the hydrogels, where green is positive and red shows a negative correlation with $p < 0.05$ in light colours and $p < 0.01$ in the darker shade.

On relating rheology and oral tribology to sensory properties in hydrogels

Emma M. Krop [a], Marion M. Hetherington [b], Melvin Holmes [a], Sophie Miquel [c], Anwesha Sarkar [a]*

[a] Food Colloids and Processing Group, School of Food Science and Nutrition, University of Leeds, Leeds LS2 9JT, United Kingdom

[b] School of Psychology, University of Leeds, Leeds LS2 9JT, United Kingdom

[c] Mars Wrigley Confectionery, 1132 West Blackhawk Street, Chicago, IL 60642, USA

*Corresponding author:

Dr Anwesha Sarkar

Food Colloids and Processing Group,

School of Food Science and Nutrition, University of Leeds, Leeds LS2 9JT, UK

E-mail address: A.Sarkar@leeds.ac.uk

Phone: +44 (0) 113 343 2748

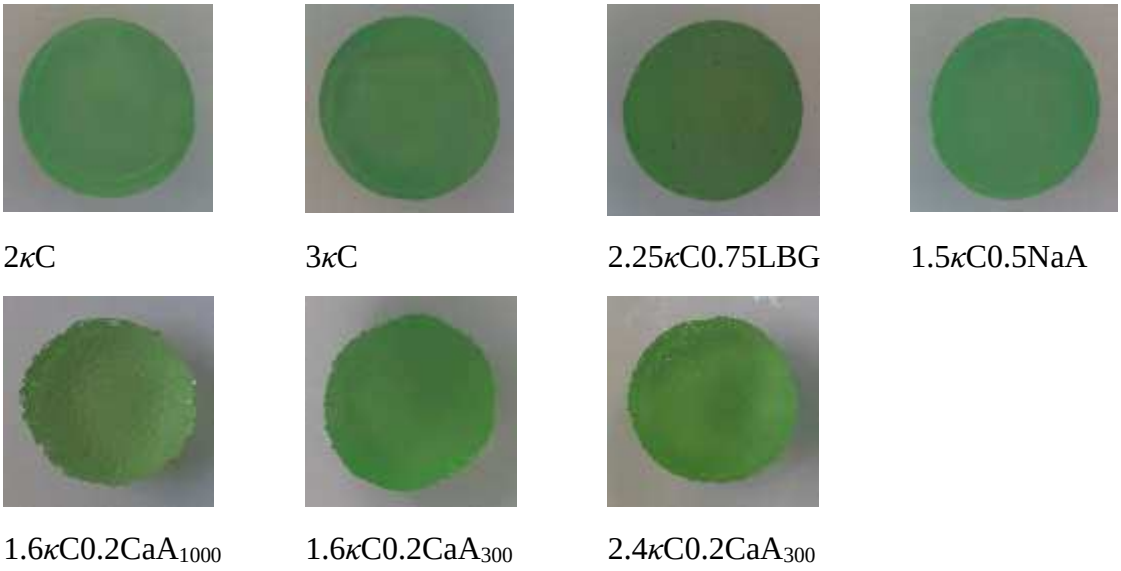

Supplementary Figure 1. Visual images of the different hydrogels.

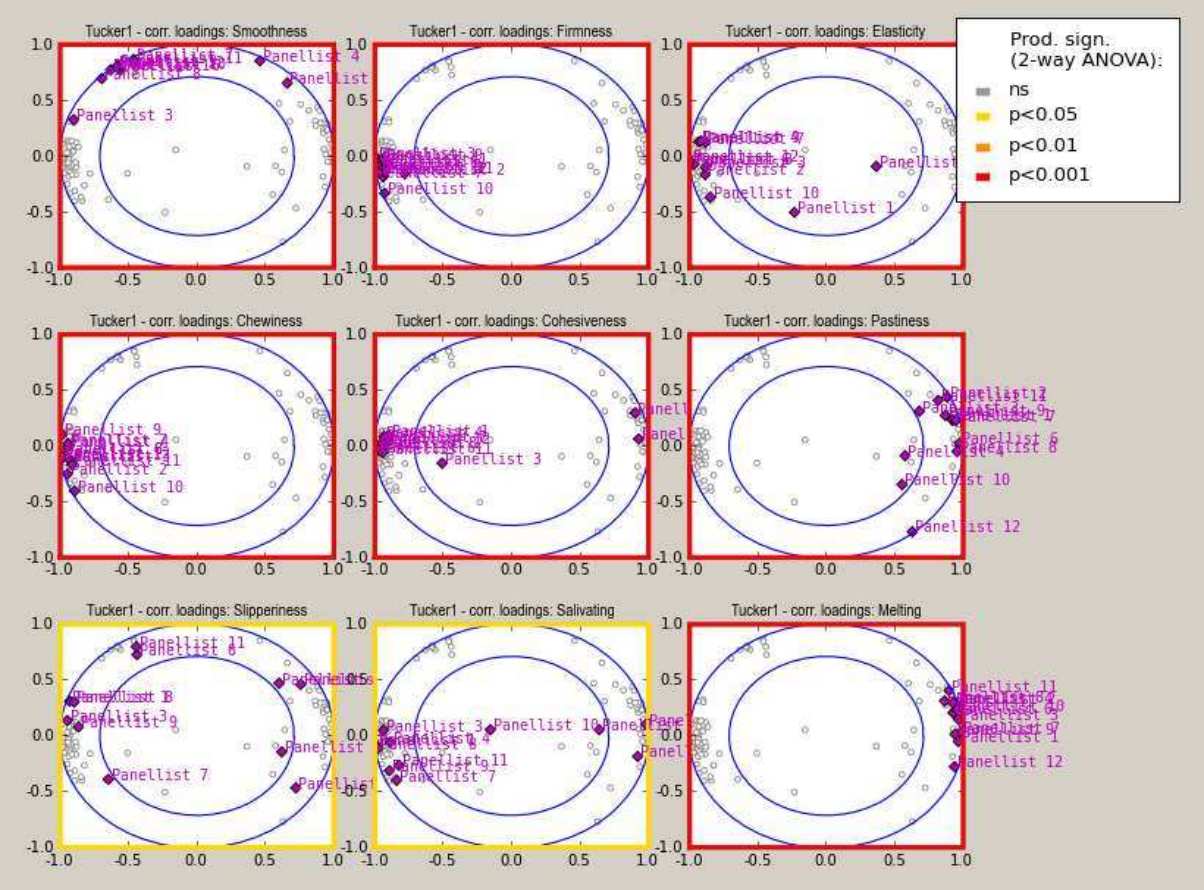

Supplementary Figure 2. Tucker-1 plots for the all attributes from the descriptive sensory analysis, showing the panel agreement.

Supplementary Table 1. Textural properties of the hydrogels obtained from uniaxial compression test. A different lower case letter denotes a statistically significant difference ($p < 0.05$).

Samples	**Fracture energy (kPa)**	
	Mean	SD
2*κ*C	91.52^{b}	8.31
3*κ*C	147.87^{a}	17.75
2.25*κ*C0.75LBG	71.13^{c}	43.74
1.5*κ*C0.5NaA	6.54^{f}	0.98
1.6*κ*C0.2CaA$_{1000}$	26.60^{e}	5.11
1.6*κ*C0.2CaA$_{300}$	22.39^{ef}	7.03
2.4*κ*C0.2CaA$_{300}$	47.27^{d}	12.85